U.S. Department of Energy
National Energy Technology Laboratory
Office of Energy Efficiency & Renewable Energy

DE-EE0006428

"Development of High-Performance Cast Crankshafts"

Final Technical Report

Author:
Mark E. Bauer, General Motors

Submitted by:
Melissa A. Smith, Contract Administrator, Caterpillar Inc.

Submission Date: April 3, 2017

Grant Recipient:
Caterpillar Inc.
14009 N. Old Galena Road
Mossville, IL 61552-7547

DUNS: 166004312

Grant Period of Performance:
1 October 2013 – 31 March 2017*

*Grant Terminated effective 31Dec2016 per Prime Contractor request

Description / Abstract

The objective of this project was to develop technologies that would enable the production of cast crankshafts that can replace high performance forged steel crankshafts. To achieve this, the Ultimate Tensile Strength (UTS) of the new material needs to be 850 MPa with a desired minimum Yield Strength (YS; 0.2% offset) of 615 MPa and at least 10% elongation. Perhaps more challenging, the cast material needs to be able to achieve sufficient local fatigue properties to satisfy the durability requirements in today's high performance gasoline and diesel engine applications. The project team focused on the development of cast steel alloys for application in crankshafts to take advantage of the higher stiffness over other potential material choices. The material and process developed should be able to produce high-performance crankshafts at no more than 110% of the cost of current production cast units, perhaps the most difficult objective to achieve. To minimize costs, the primary alloy design strategy was to design compositions that can achieve the required properties with minimal alloying and post-casting heat treatments.

An Integrated Computational Materials Engineering (ICME) based approach was utilized, rather than relying only on traditional trial-and-error methods, which has been proven to accelerate alloy development time. Prototype melt chemistries designed using ICME were cast as test specimens and characterized iteratively to develop an alloy design within a stage-gate process. Standard characterization and material testing was done to validate the alloy performance against design targets and provide feedback to material design and manufacturing process models.

Finally, the project called for Caterpillar and General Motors (GM) to develop optimized crankshaft designs using the final material and manufacturing processing path developed. A multi-disciplinary effort was to integrate finite element analyses by engine designers and geometry-specific casting simulations with existing materials models to optimize crankshaft cost and performance. Prototype crankshafts of the final design were to be produced and validated using laboratory bench testing and on-engine durability testing.

ICME process simulation tools were used to investigate a broad range of processing concepts. These concepts included casting orientation, various mold and core materials, and various filling and feeding strategies. Each crankshaft was first simulated without gating and risers, which is termed natural solidification. The natural solidification results were used as a baseline for strategy development of each concept. Casting process simulations and ICME tools were proven to be reasonable predictors of real world results.

Potential alloys were developed that could meet the project material property goals with appropriate normalization and temper treatments. For the alloys considered, post-normalization temper treatments proved to be necessary to achieve the desired yield strengths and elongations and appropriate heat treatments were designed using ICME tools. The experimental data of all the alloys were analyzed in combination with ICME tools to establish chemistry-process-structure relations.

Several GM small gas engine (SGE) crankshafts were successfully cast in sand molds using two different sprue, runner, gate, riser, chill designs. These crankshafts were cast in two different steel alloys developed during the project, but casting finishing (e.g. riser removal) remains a cost challenge.

A long list of future work was left unfinished when this project was unexpectedly terminated.

Keywords

cast, casting, steel, alloy, crankshaft, material, property, ICME, temper, tensile, yield, elongation, GM, Caterpillar

Project Objectives

- To improve the power density of today's gas and diesel engines, material and process technologies will be developed that will enable the production of cast crankshafts that meet or exceed the performance of current state-of-the-art high performance forged crankshafts.
- To achieve minimum core material properties of 850 MPa Ultimate Tensile Strength (UTS) and 615 MPa Yield Strength (YS) with at least 10% elongation. Material must also be able to meet the local ultra-high cycle fatigue properties required in a crankshaft.
- To identify a pathway to meet incremental cost targets of less than 110% of current production cast units.

Project Approach

- An Integrated Computational Materials Engineering (ICME) approach was utilized to computationally engineer new material compositions and manufacturing processes to achieve improved performance of cast steel alloys.
- Process-structure modeling techniques were to be integrated with finite element analyses by crankshaft designers to optimize crankshaft life cycle cost and performance.
- Prototype melts were produced and characterized iteratively for an alloy design within a stage-gate process to validate the alloy performance and provide feedback to material design and manufacturing process models.
- The Advanced Photon Source (APS) at Argonne National Labs was to be utilized to conduct innovative in-situ measurements of phase evolutions and damage during heating and cooling under various loading conditions.
- Production and validation of prototype crankshafts was to be performed using standard bench tests at Caterpillar and GM. A full engine test was planned for the prototypes to test the crankshaft and con-rod bearing system.

2014 Accomplishments

- Defined common material requirements and validation procedures for Caterpillar and GM crankshafts.
- Identified and prioritized alloy, processing, and design concepts for investigation.
- A tapered cylinder test bar casting design for future Design of Experiments was completed and optimization of approximately a half dozen alloy concepts was in progress. Full characterization of an initial baseline alloy casting trial was underway.

- Baseline castability studies of current crankshaft designs were begun. Investigation of innovative methods for producing clean steel castings with casting process simulation models was underway.

2015 Accomplishments

- ICME based alloy design was completed and a matrix of 14 alloys was developed to evaluate the initial concepts.
- Casting trials were completed for ten of the fourteen alloys in the initial alloy matrix.
- Structure and property characterization was completed for eight of the ten alloys produced through the end of 2015.
- Simulation based evaluation of several casting concepts was completed. A horizontal orientation casting concept was fully developed and two prototype crankshaft castings were produced using 3D printed sand molds.
- A Vacuum-Assisted Counter-Gravity (VACG) system was designed and fabricated for laboratory scale casting trials.

2016 Accomplishments

- Casting trials of test samples (bars and keel blocks) was completed for 12 alloys.
- Tensile tests were carried out for the 12 alloys in different conditions [as-cast, normalization, normalization and temper, or quenching and temper].
- Microstructure, phase constituents, grain size, micro-porosity, and fracture surface were examined for the test samples in connection with mechanical properties.
- Dilatometry analysis was conducted to investigate phase transformation at different cooling rates for alloys 2, 6, 7, and 10.
- A temper heat treatment study indicated weak effect at 225^{o}C, but strong effect at 500^{o}C which leads to slight variation of UTS, certain increase of YS, and significant increase of elongation.
- Alloys 3, 4, 6, and 8 can meet the goals (UTS>850 MPa, YS>615 MPa, elongation>10%) after normalization at 1050^{o}C for 1 hour and temper at 500^{o}C for 4 hours.
- Alloys 10 and 11 can also meet the goals, but they may not have sufficient hardenability for induction hardening due to low C.
- Alloys 12, 13, and 14 have low yield strengths for the heat treatments considered and could not meet the goals.

Remaining Milestones at time of project termination notice

nearly completed:

- Refine design of high-potential (HP) alloy concepts

partially completed:

- Refine design of high-potential (HP) processing concepts
- Develop initial crankshaft design concepts & FMEA based on HP alloys and processes

- Evaluate castability of HP alloys (fluidity & hot tear experiments)
- Pour prototype castings
- Evaluate prototype casting quality and location specific properties
- Prototype high-potential alloys and processes (single crankpin scale model or full crankshaft)
- Evaluate casting quality & mechanical properties of sample HP castings
- Virtual optimization of prototype crankshaft design considering final alloy properties
- Optimize casting and heat treat processes for final prototype using ICME

not started:

- Evaluate local processing effects (induction hardening, fillet rolling, etc.)
- Generate complete property dataset for design and FEA/simulation
- Machining and heat treatment of prototype crankshafts
- Evaluate machinability of final alloy design and machining cost model
- Prototype cast crankshaft validation - bench testing
- Prototype cast crankshaft validation - on-engine testing
- Variation analysis and allowables prediction (material, process, performance)
- Cost model for new material and manufacturing value stream vs. baseline

Introduction

Vehicles of the future need to meet increasing fuel efficiency standards with low exhaust emissions while meeting the performance and cost expectations of consumers. This is true whether considering light-duty automotive or heavy-duty vehicle segments. A vehicle's power source is a critical component in meeting these objectives. Engine manufacturers will need to produce engines that are lighter weight and operate in more efficient combustions regimes in order to deliver fuel efficiency, emission, and power requirements. Increasing the power density of the engine is thus a direct approach to achieving these objectives. However, increasing engine power and efficiency requires higher operating cylinder pressures, resulting in increased loads on the crankshaft. For higher performance applications, the loads on the crankshaft are too high for today's cast materials and thus are required to be produced from more expensive steel forgings. Enabling the use of cast crankshafts for high-performance engines will enable designers at GM and Caterpillar to optimize material utilization to develop lighter weight crankshafts while maintaining the torsional and bending stiffness requirements. Reducing the rotating mass of the crankshaft will enable further reduction in the engine block weight as it supports the crankshaft loads. Replacing current cast ductile iron crankshafts used in smaller engines with higher strength castings will enable the power and efficiency of the engine to be increased. Thus, smaller more efficient engines may be able to replace larger engines, which could greatly reduce the demands on petroleum resources and the amount of greenhouse gasses emitted annually from automobiles and heavy duty trucks and equipment.

The objective of this project was to develop technologies that would enable the production of cast crankshafts that can replace high performance forged steel crankshafts. To achieve this, the Ultimate Tensile Strength (UTS) of the new material needs to be 850 MPa with a desired minimum Yield Strength (YS; 0.2% offset) of 615 MPa and at least 10% elongation. Perhaps more challenging, the cast material needs to be able to achieve sufficient local fatigue properties to satisfy the durability requirements in today's high performance gasoline and diesel engine applications. The material and process developed should be able to produce high-performance crankshafts at no more than 110% of the cost of current

production cast units.

The project team focused on the development of cast steel alloys for application in crankshafts to take advantage of the higher stiffness over other potential material choices. The current alternative material for cast crankshafts, ductile iron, has a lower Young's Modulus than steel (typically 14% lower), which results in a significant drop in crankshaft stiffness if mitigating redesign (addition of more material) is not considered. The drop in stiffness leads to increased force transmission into the cylinder block which can lead to not only structural implications, but also an increase in noise levels. Utilizing the casting process and the stiffness advantage of steel will allow the weight reduction potential to be maximized without sacrificing performance.

The significant challenge in this project was developing production methods for steel castings that can meet the performance and cost requirements. To minimize costs, the primary alloy design strategy was to design compositions that can achieve the required properties with minimal alloying and post-casting heat treatments. The team explored approaches to achieve higher strength microstructure phases from lower cooling rates, optimizing the solidification freezing range, refining the solidification grain structure, and precipitating nanostructures that strengthen and improve the toughness of the material. New filling, feeding, and molding techniques were investigated to achieve the desired liquid metal flow and solidification behavior to yield castings with minimal porosity and inclusions.

An Integrated Computational Materials Engineering (ICME) based approach was utilized, rather than relying only on traditional trial-and-error methods, which has been proven to accelerate alloy development time. Prototype melt chemistries designed using ICME were cast as test specimens and characterized iteratively to develop an alloy design within a stage-gate process. Standard characterization and material testing was done to validate the alloy performance against design targets and provide feedback to material design and manufacturing process models.

Prototype crankshafts were then to be produced using the high-potential material and processing concepts developed in this project. Additional manufacturing processes required to resist cyclical bending and torsional stresses, especially in the concentrated stress regions like the bearing journal fillets and oil drill holes, were then to be investigated. Imparting compressive residual stresses into the part is a potential method for mitigating stresses and reducing potential material development risks.

Finally, the project called for Caterpillar and GM to develop optimized crankshaft designs using the final material and manufacturing processing path developed. A multi-disciplinary effort was to integrate finite element analyses by engine designers and geometry-specific casting simulations with existing materials models to optimize crankshaft cost and performance. Prototype crankshafts of the final design were to be produced and validated using laboratory bending and torsion tests. A full engine test was planned on a running engine for a specified duration with periodic measurements to determine durability and reliability. The on-engine test was also to qualify that the crankshaft and con-rod bearing system would withstand severe operating conditions.

In addition to the resources at Caterpillar and GM, the project benefited from the expertise of other project collaborators.

Northwestern applied its Integrated Computational Materials Design (iCMD) toolset, Figure 1, which is a core modeling software system that integrates proprietary and commercial mechanistic modeling tools to facilitate rapid design and development of new materials, and has been demonstrated on many novel

steels. For solidification and solid-state transformation modeling, the iCMD platform includes the proprietary multicomponent multi-particle precipitation code, PrecipiCalc™ which draws upon calculations from CALPHAD software tools such as Thermo-Calc® and DICTRA for thermodynamic and diffusion information.

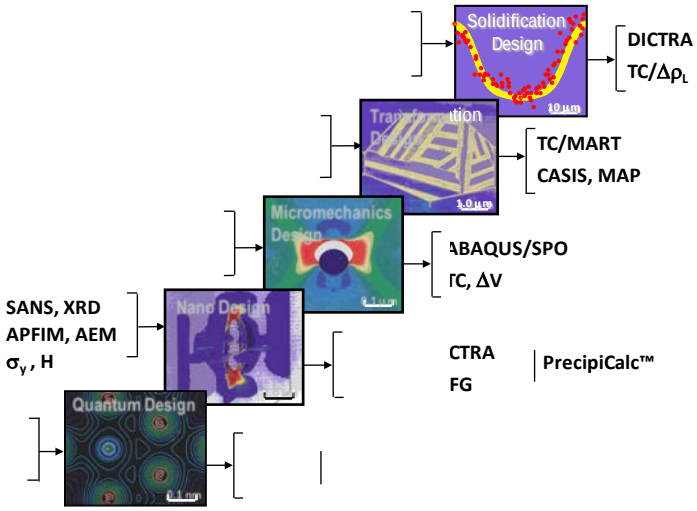

Figure 1: Hierarchy of design models supporting computational materials design. Acronyms at right are models and software platforms. Acronyms at left are instrumentation employed for calibration and validation.

The University of Iowa has developed advanced casting process simulation models for calculating porosity and inclusion formation in steel castings. These models quantitatively predict the size of the defects that can then be mapped into fatigue models to predict the effect on the life of the casting and can be used to optimize casting design and quantify allowable defects such as micro-porosity.

Argonne National Lab has an Advanced Photon Source (APS) that can quantify casting quality and conduct innovative in-situ measurements of phase evolutions and damage nucleation during thermal and mechanical loading conditions to better understand chemistry-structure-process relationships.

Alloy Development

For a cast steel alloy, solidification takes place in liquid region around 1500°C, while solid transformation occurs around 705°C, at which the cooling rate would give the most significant impact on the final transformation microstructure for a given composition. Thus, the microstructure and performance of an alloy not only depend on chemical composition, but also on heat treatment after casting. Optimization of the initial alloy concepts was performed using various ICME tools. The first step was to simulate the casting and heat treat processes for a representative crankshaft to determine the cooling rates at the critical temperatures. Figure 2 shows the casting orientation and locations of virtual thermal-couples which are set to examine their cooling rates during solidification and heat treatment. For the baseline case, the casting was solidified in a sand mold and shaken out after 8 hours, followed by austenization at 950 °C and air cooled to 50°C. The cooling rates at the virtual thermocouples at 704°C were around 0.02°C/s during solidification and in mold cooling and between 0.3°C/s and 0.4°C during austenization and cooling in still air.

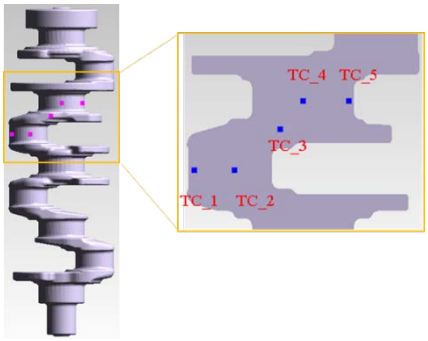

Figure 2. Typical crankshaft geometry with section view showing location of virtual thermocouples.

The next step was to examine the effect of alloying elements on structure formation and mechanical properties. In this approach, for each concept a base composition is selected and elements of interest are selected as design variables with ranges specified based on cost, solubility, and other thermodynamic factors. The design optimization was iterative in nature, where each design variable was adjusted independently while holding the other elements in the composition constant. A cooling rate of 0.4°C was then used for calculations of the microstructure phases and properties through the defined range for each design variable. Figure 3 shows an example of the calculated results for the effects of *C* and *Mo* on bainite transformation for a given steel at three different *Mn* concentrations. It was seen that *C* had less effect when Mn was above 1.4%, while *Mn* exhibited strong effect until its addition reached 1.4% and was most influential for lower *C* levels. *Mo* additions were seen to strongly influence bainite formation. The degree of the *Mo* effect changed not only with its addition, but also with *Mn* content in the steel. As a consequence, it was better first to determine levels of *C* and *Mn* and then determine the *Mo* level based on the structure-property requirements.

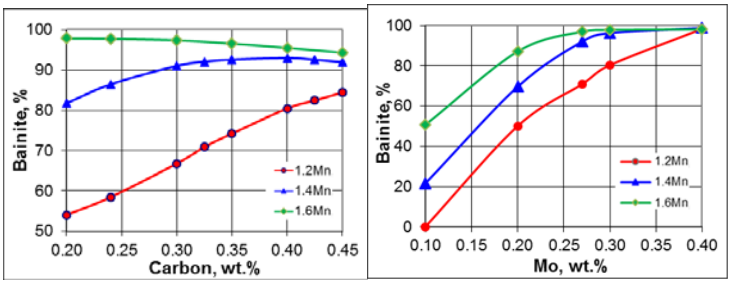

a) **b)**

Figure 3. a) Effect of carbon and b) effect of molybdenum on bainite transformation in steel.

Mechanical properties are calculated using JMatPro based on the predicted phase fraction. Calculations have shown that JMatPro predicts the same trend for both yield strength and tensile strength for a given steel at a certain cooling rate. For simplicity, examples of the effect of alloying elements on yield strength only are presented. Figure 4 shows the effect of *C* on the calculated yield strength for a given steel at three different *Mn* levels. It is seen that addition of *C* leads to a linear increase of yield strength within a wide composition range. A similar effect is also predicted for *Mo*.

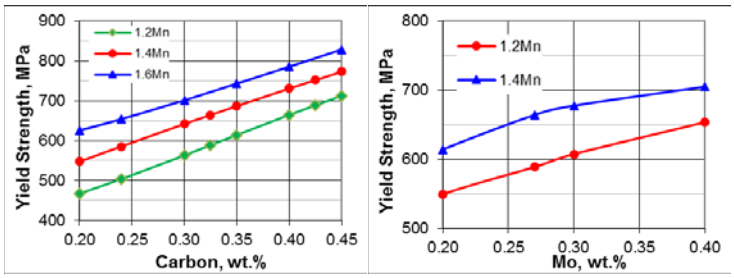

a) **b)**

Figure 4. a) Effect of carbon and b) effect of molybdenum on the yield strength in steel.

In addition to designing alloys with primary phase fractions needed to meet the strength requirements through only air cooling, low carbon steels with good castability were investigated that relied on precipitation hardening processes to achieve strength requirements. The current design concepts adopted the same strengthening concept from Blastalloy160 steel developed Prof. Greg Olson's research group at Northwestern University, which relies on precipitation of coherent *Cu* and M_2C, i.e. *(Mo,V)$_2$C* carbide phases. In order to improve toughness, grain refining of the cast alloy was an important step. Strategic formation of MC carbides were investigated to assist in pinning the grains during subsequent heat treatment which would help refine the grains. Inoculation strategies were also investigated to assist in heterogeneous nucleation of ferrite or austenite grains. Toughness was also significantly impacted by the formation of micro-porosity, carbo-nitrides, and other non-metallic inclusions. Nitrogen content during melting needed to be controlled, which can be difficult, as excess N leads to micro-porosity and embrittling phases. Step diagrams were calculated to optimize the composition and processing path for desired precipitate formation. Figure 5 shows example step diagrams for different nitrogen levels in a particular steel composition. It can be seen that *N* strongly influences the *V(C,N)* formation, which is significant for high *N*. It should be noted that the processing temperatures and times would be further revised according to initial experimental results. For example, by controlling temper time, it is possible to study the kinetics of precipitate nucleation and coarsening.

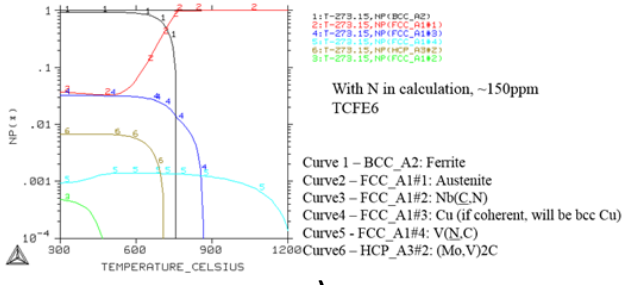

a)

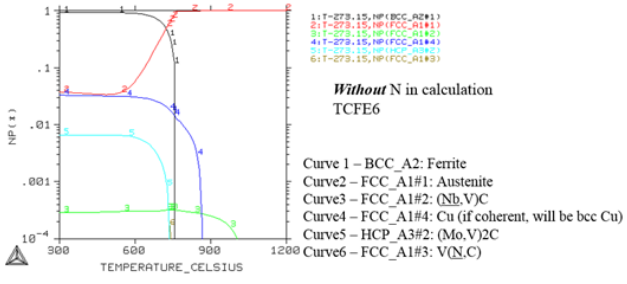

b)

Figure 5. Example step diagrams for a given steel alloy concept. a) 150 ppm N, b) 0 ppm N.

Preliminary trials were conducted using a modified SAE 15V22 steel alloy to cast weld-plates with dimensions of 184x305x34 mm, as shown in Figure 6. Figure 6(b) shows the thermocouple locations used in the simulations in order extract the cooling rates in the plates during solidification and heat treatment. The plates were normalized following casting by austenitizing at 950°C for 1 hour followed by either a still air-cool or fan cool to room temperature. The simulation indicated that the cooling rate at all locations around 700°C is about 0.035°C/s during solidification, while cooling rate during normalization depends on location as follows: Corner (TC-2): ~0.50°C/s, Edge (TC-1, TC-5, TC-6): ~0.40°C/s, Center (TC-4): ~0.30°C/s.

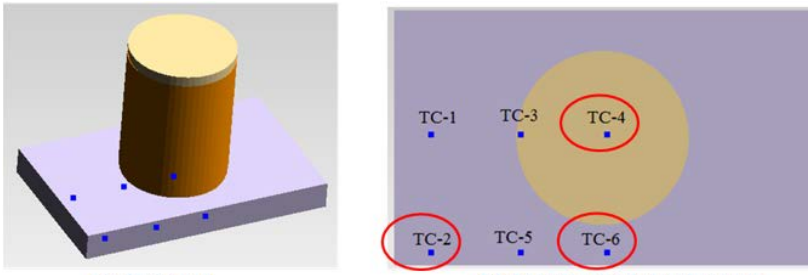

Figure 6. Cast setup of weld-plate with dimension of 184x305x34 mm. The marks are locations of virtual thermocouples set in the simulation.

Tensile specimens were taken from the edge of the plates (TC-5/6 location) and Charpy specimens were taken from the corner of the plates. The mechanical test results are listed in Table 1. JMatPro was used to predict microstructure phases and mechanical properties in the weld plate using cooling rates from solidification and normalization simulations and those predictions are presented in Table 2.

Table 1. Mechanical properties of weld-plate cast with modified SAE 15V22.

1E1667mod	1A	1B	2A	2B
Solution at 950°C	Normalization with air-cool	Normalization with fan-cool	2x Normalization with air-cool	2x Normalization with fan-cool
Tensile, MPa	853, 784	839, 801	833, 760	855, 800
Yield, MPa	581, 582	577, 586	575, 570	585, 591
Elongation, %	3, 2	3, 1.3	3.2, 2.1	3.1, 2.2
RA	5, 5	5, 4	6, 4	4, 4
Charpy-V at room temp	11.8, 10.9, 10.9	11.5, 10.6, 11.8	15.1, 12.9, 16.4	13.7, 13.6, 12.6
HRC surface	26, 27, 27	27.5, 28, 27.5	26.5, 26.5, 26.5	28, 27.5, 27.5

Table 2. Comparison of different predictions with experiments of mechanical properties of weld-plate cast with modified SAE 15V22.

Location	Cooling Rate (around 700°C)	Phases %		Properties after Normalization		
		Bainite	Pearlite	YS (Mpa)	UTS (Mpa)	HRc
TC-2: Corner	0.5°C	99	1	663	911	27.7
TC-6: Side	0.4°C	98	2	654	901	27.2
TC-4: Center	0.3°C	95	4	643	888	26.5

The plate casting used for the preliminary alloy trial discussed above had a large riser in the middle of the plate as shown in Figure 6. Since the plate is not very thick, test specimens could not be taken from regions under the riser as they would have been too close to the riser. The large riser would lead to

significant under riser segregation which was not desirable for evaluating different alloy concepts. Thus the team focused on developing a new test casting design to produce samples in support of the alloy development effort. A key requirement for the test casting was to have sections with varying cooling rates during solidification and heat treatment that are representative of the range of cooling rates that an actual crankshaft would experience. Calculated cooling rates in a small Caterpillar crankshaft ranged from 0.5°C/s to 2.5°C/s during solidification and were around 0.02°C/S at the solid-state transformation temperature during in-mold cooling. After normalization, the cooling rates were between 0.3°C/s and 0.4°C/s at the solid-state transformation temperature during air cooling.

Based on ICME materials design work, a test matrix of 14 alloys was developed. The microstructure phases (B – Bainite, F – Ferrite, P – Pearlite and M- - Martensite) and the mechanical properties shown in Table 3 were predicted using the ICME software JMatPro and represent air cooling at 0.4°C/s. Two of the alloys are industry standard grades and one is a standard micro-alloy forging steel. Three of the alloys are duplicate compositions, but have a grain refiner addition during the melting and treatment process. It was not possible to predict the effect of the grain refiner on the mechanical properties, however the aim was for the biggest effect to be increasing toughness, which is not a property that can be predicted with ICME tools today.

Table 3. Preliminary alloy test matrix.

Steel	Designation	Phases				YS	UTS	HRc
		B	F	P	M	MPa	MPa	
1	V-MA650-1	97.8	0.5	1.7	--	654	901	27.2
2	V-MA650-2	86.4	8.4	27.0	--	650	889	27
3	V-MA650-2 +GR							
4	V-MA650-3	72.6	15.0	12.4	--	662	910	27.6
5	V-MA650-3 +GR							
6	SiV-MA700	31.1	14.2	54.8	--	707	959	30
7	SiV-MA650	36.2	30.5	33.4	--	661	902	27.6
8	SiBo Steel	17.7	9.9	1.1	71.1	1364	1603	49.8
9	SiBo Steel +GR							
10	NU-Cast1000	98.8	0.01	--	1.24	1024	1283	42
11	NU-Cast700	86.2	13.8	--	--	724	977	30.8
12	4140	82.9	16.2	0.9	--	656 635*	903 972*	27.3 30*
13	GM 1538MV	--	19.2	80.8	--	531	761	19.2
14	1330							

* 2” round bar wrought material (normalization at 870°C, air-cooling) from matweb: http://www.matweb.com

The project explored approaches such as adjustment of compositions and different heat treatments to achieve higher strength microstructure phases from lower cooling rates, optimizing the solidification freezing range, refining the solidification grain structure, and precipitating nanostructures that strengthen and improve the toughness of the material.

Casting of Test Samples and Crankshafts

Test samples of most designed alloys were cast with sand molds in the following foundries.

- STL: St. Louis Precision Casting Company, St. Louis, MO
- SCP: Southern Cast Products, Jonesboro, AR
- HUR: Huron Casting Inc., Pigeon, MI

The cast samples were made in bar shape as shown in Figure 7, or as keel blocks shown in Figure 8.

The test bar mold was developed using three bars in each mold with nominal diameters of 1", 2", and 3", as seen in Figure 7. Each test bar was tapered to promote directional solidification toward the top, where a large head acted as a riser to feed metal during solidification to minimize porosity. The bars were filled from the bottom to promote a smooth non-turbulent filling to reduce the formation of reoxidation inclusion defects. Cooling rates were calculated at around 704°C at the center of each bar. During in-mold cooling after solidification, the cooling rates varied from 0.03 to 0.04°C/s, while they ranged from 0.29°C in the 3" bar to 0.45°C in the 1" bar during air-cooling after normalization. These values represented very well the predicted cooling rates at different locations in the Caterpillar01 and GM crankshafts previously analyzed.

As results of the mechanical testing were becoming available, the elongations of several of the alloys were lower than required. Examination of the fracture surfaces revealed micro-porosity, too small to be seen on X-rays, was present in many tensile specimens. This possibility was expected for specimens taken from the centerline of the bars, but micro-porosity was also present in specimens extracted off-centerline. Thus, the team decided to start casting keel block samples as shown in Figure 8 in addition to the tapered cylinder test bars. The advantage of the keel block was that the "legs" were fed from the top block within very short distance which minimizes the potential for micro-porosity formation. Original keel block legs were cast in traditional single keel block molds producing two "legs" available for tensile bar blanks. Later, a pattern and molding boxes were developed that cast four keel blocks in each mold as shown in Figure 8(a), and each keel block had an additional top riser to ensure sound "legs." Each keel block had two "legs" where tensile bars were extracted as illustrated in Figure 8(b). All keel blocks cast after 9 March 2016 used the four-on keel block molds.

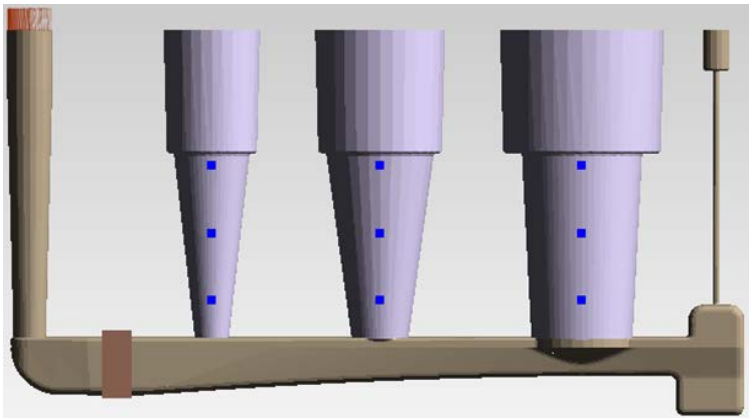

Figure 7. Final design of test bar casting with gating system and riser heads.

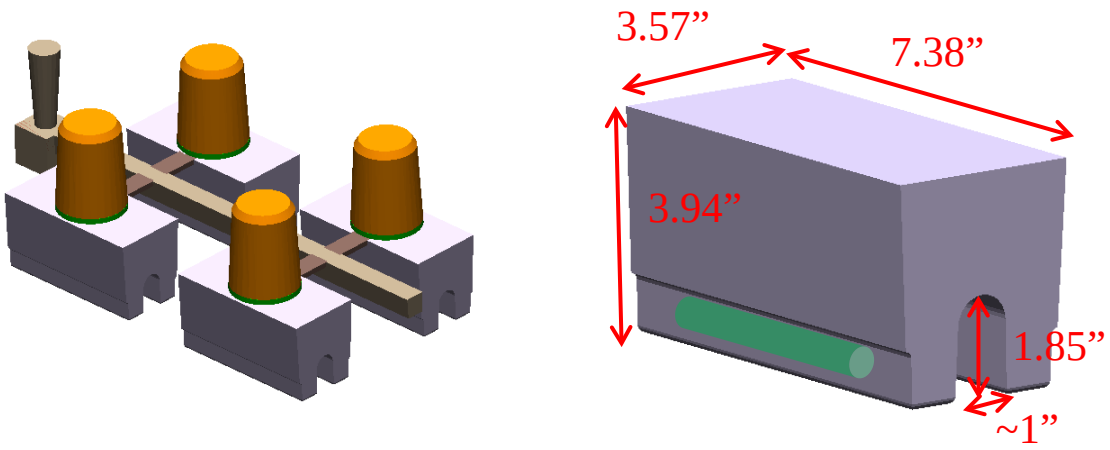

a) Cast setup of keel blocks b) Location of tensile bars

Figure 8. Cast setup of keel blocks (a) and location of tensile bars in keel block (b).

In addition, two prototype crankshafts were also cast in alloy 2 at St. Louis Precision Casting Company using a rigging designed by the University of Iowa based on a series of cast simulations with different orientations, riser placements and contact areas, application of chills, etc. The final sand cast rigging used a horizontal orientation and fed the crankshaft through a riser attached to the flange end. The overall mold yield was 34.3% due to the large volume of required risers. As shown in Figure 9, three tensile bars were excised from the GM crankshaft cast in alloy 2 at St. Louis Precision Casting: one from the flange end (F), one from the section between pin journal 2 and main journal 3 (C), and one from the stem end (P).

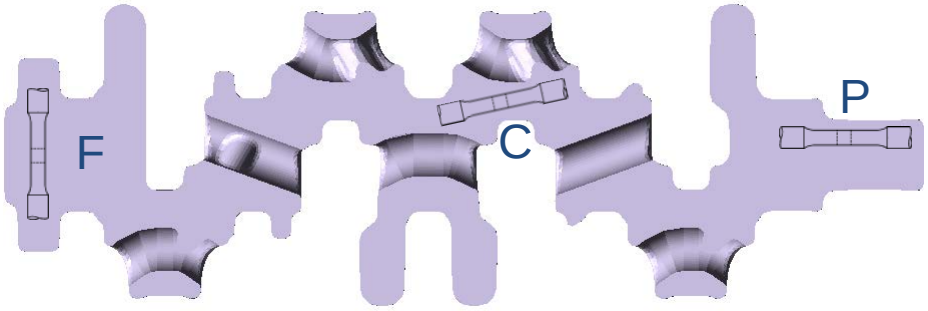

Figure 9. Location of tensile bars in the crankshaft.

Material Property Analysis

For each alloy, initially two test bar molds were cast and cooled in the mold overnight and then shaken out and shot blasted to remove any stuck on sand. The test bars were then cut off the runner bar and shipped to Caterpillar’s Technical Center where all the 1” and 3” test bars were normalized for three hours at a specifically defined temperature for each alloy. All the normalized bars were removed from the furnace and cooled in still air. The 2” bars were left in the as-cast condition. After heat treatment, one set of bars for eight of the ten alloys produced was sent to Element Materials Technology for

metallurgical and mechanical property characterization. Two sets of bars from alloys 12 and 14 were sent to Element as one set of each of these alloys had a quench and temper process performed to compare against the samples in the normalized and as-cast conditions. Samples for two of the alloys were sent directly to Northwestern for optimal heat-treatment determination.

The 1" heat treated bars had low elongations due to micro-porosity at the centerline of the bars. In some cases, the properties of these bars were not much different than the as-cast condition. This indicated that micro-porosity was likely dominating the properties, making it difficult to directly compare the alloys at this location. Tensile specimens were then extracted from a mid-radius location in the 3" bars. The ultimate tensile strengths and elongations at this location were higher than at the centerline due to less micro-porosity; however, some micro-porosity was still present which resulted in low elongation results even for the mid-radius bars. Despite the micro-porosity, several of the alloys had tensile strengths near the target in 3" bars, namely alloys 2, 3, 6, and 12. To better make a direct comparison of material properties, keel blocks were cast for the most promising alloys. Tensile strength and elongation targets (850 MPa UTS, 10% Elongation) were achieved on average in alloy 2 keel blocks. This alloy was thought to be a leading candidate and was chosen for prototype crankshafts cast at St. Louis Precision Casting Company.

In early January 2016, Huron Casting finished poured the second of two heats intended to determine if the observed porosity and lower than expected mechanical properties for alloy development castings made at St. Louis Precision Casting were an artifact of their specific metal handling practices or not. The idea was to compare the results for castings poured at St. Louis Precision's job shop directly from the melting furnace to castings poured at a large production steel pouring operation from a teapot ladle. It was concluded that the metal preparation and pouring practices at St. Louis Precision were not the cause of lower than expected mechanical properties.

Heat treatments for alloys 1 through 8 during the initial studies were focused only on normalization. The cast samples were normalized at temperatures around 900^{o}C for 1-3 hours followed by cooling in still air. Then tensile tests were carried out, and hardness was measured. Microstructures, phase constituents, grain size, micro-porosity, and fracture surfaces were also examined. Alloys 10 and 11 were treated with water quenching and temper, and microstructure was analyzed after each heat treatment. Dilatometry analysis was also conducted by Northwestern University to investigate phase transformation at different cooling rates for alloys 2, 6, 7, and 10. Alloys 12, 13, and 14 were treated with normalization or water or oil quenching and tempering. Then similar tests and analysis were carried out as for alloys 1 through 8.

Results of tensile testing and analysis of porosity, grain size, and microstructure for all samples in the normalized condition were studied and the following observations were made:

(1). Keel blocks have best properties, especially elongation.
(2). Tensile bars excised from the mid-radius section of 3" bars had the best properties of the test bars samples, and those properties were comparable to corresponding keel block samples.
(3). Samples from the center of 1" and 3" bars exhibited low elongation, most likely due to micro-porosity.
(4). Some samples from alloys 2 through 8 satisfied the UTS (>850 MPa) and elongation (>10%) goals, but their yield strength was slight lower than the goal 615 MPa.
(5). Alloy 1 has low strength due to low carbon.
(6). Alloys 12, 13, and 14 had low yield strength or low elongation, and did not meet the goals.

(7). Only a few of the alloys were at or near the minimum yield strength target of 580 MPa. Many of the microstructures did not exhibit significant changes from the as-cast microstructure after normalization. This indicated the alloys may not have been optimized for achieving the required microstructure under air cooling conditions or that the normalization time and temperature required further optimization. Dilatometry and X-ray diffraction experiments were begun to develop CCT and TTT curves for the higher potential alloy candidates for use in ICME tools to optimize the alloy composition and heat treatment to achieve desired structures.

(8). The GM crankshafts cast in alloy 2 at St. Louis Precision Casting on 6 August 2015 were normalized at 900°C for 3 hours and cooled in still air. Three tensile bars were excised from one of the crankshafts and had the very promising properties shown in Table 4 (reference Figure 9). Note that keel block legs cast in alloy 2 in early and later stages of the project showed some promise, but generally the results from keel blocks didn't come close to the combination of UTS and elongation properties measured in the bars excised from the crankshaft casting.

Table 4. Properties from tensile bars excised from a GM SGE crankshaft cast in alloy 2 then normalized

tensile bar location (reference Figure 9)	**UTS (MPa)**	**YS (MPa)**	**Elongation (%)**
flange end (F)	915	582	17.2
section between pin journal 2 and main journal 3 (C)	894	570	14.1
stem end (P)	916	598	16.3

From the above analysis it was observed that the samples from 3" mid-radius bars and keel blocks produced the best results, and hence they were used for further comparisons and analysis including the results of post-normalization temper treatments. Since the test specimen yield strengths were lower than the goal, more heat treatments such as fan cooling and tempering were studied to assess their effects on strength and ductility.

Dilatometry Analysis

Dilatometry analysis was conducted by Northwestern University to investigate phase transformation at different cooling rates for alloys 2, 6, 7, and 10. Figure 10 shows the results of alloy 2 at cooling rates of 20K/s and 0.4K/s, respectively. From the curves' transformation temperatures, the amount of each phase after cooling down to room temperature could be estimated. It was seen that the microstructure consisted of martensite and bainite in alloy 2 at a cooling rate of 20K/s, while it consisted of ferrite, pearlite, and bainite at a cooling rate of 0.4K/s. The notations of transformation temperatures are abbreviated as follows.

Ac1: Austenite begins to form during heating
Ac3: Completion of the transformation from ferrite to austenite during heating
Ms: Start transformation temperature of martensite during cooling
Bs: Start transformation temperature of bainite during cooling
Tf: Start transformation temperature of ferrite during cooling
Tp: Ferrite ends and pearlite starts during cooling
Ar1e: Pearlite ends during cooling

A Continuous Cooling Transformation (CCT) diagram was then constructed for alloy 2 based on the dilatometry analysis in combination with ICME calculations and is presented in Figure 11. This was used as a guide for selection of temper treatment.

Dilatometry measurements for alloy 6 are presented in Figure 12 at different cooling rates. In comparison with alloy 2, alloy 6 transforms to almost full martensite at 20K/s due to its higher hardenability, as shown in Figure 12(a). On the other hand, the transformation involves ferrite, pearlite, and bainite at 0.4K/s as indicated in Figure 12(b). A CCT diagram was also constructed for alloy 6 in the same way as alloy 2 and is shown in Figure 13.

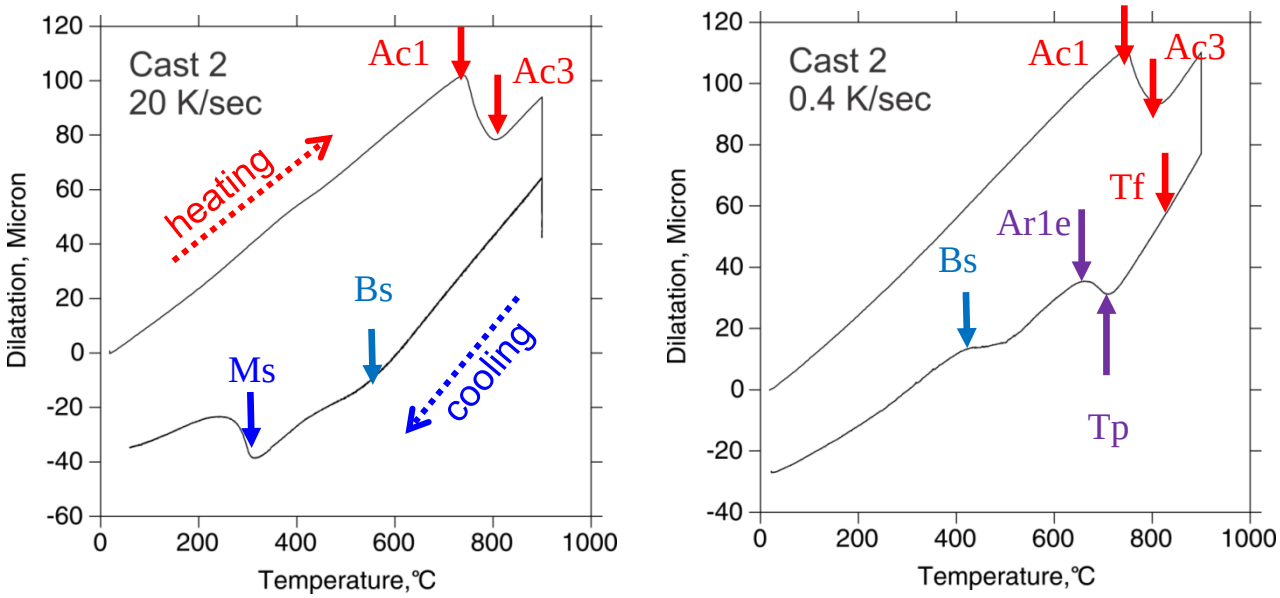

a) Cooling rate 20K/s **b) Cooling rate 0.4K/s**

Figure 10. Dilatometry measurements of alloy 2 at different cooling rates.

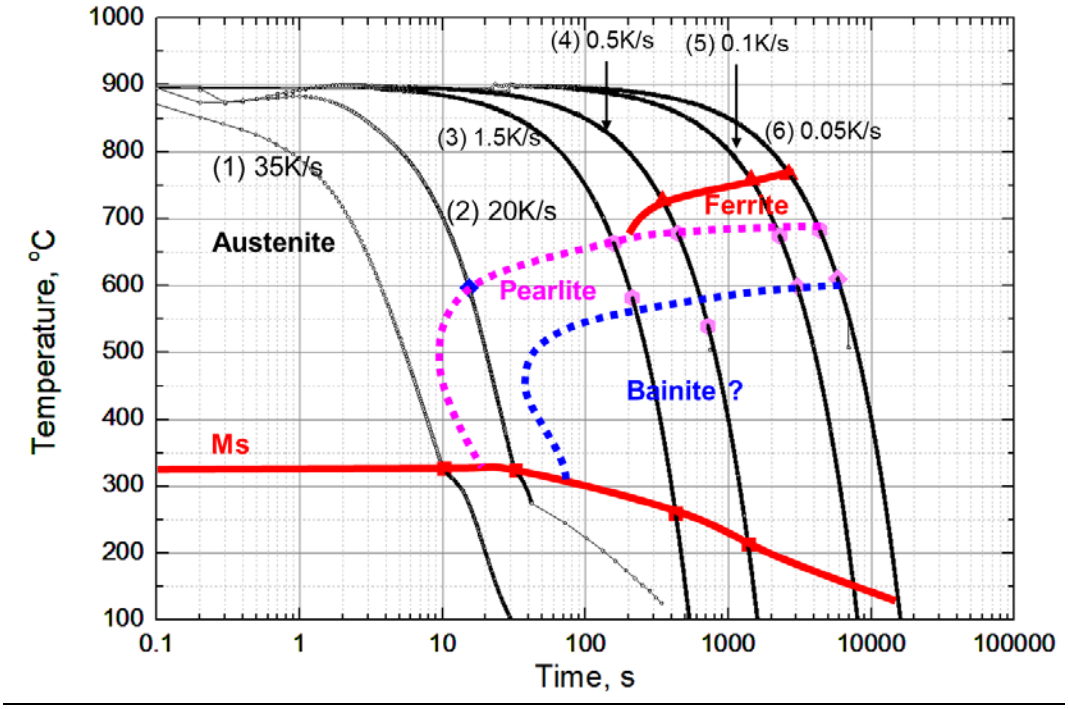

Figure 11. CCT diagram of alloy 2 constructed based on dilatometry measurements at different cooling rates

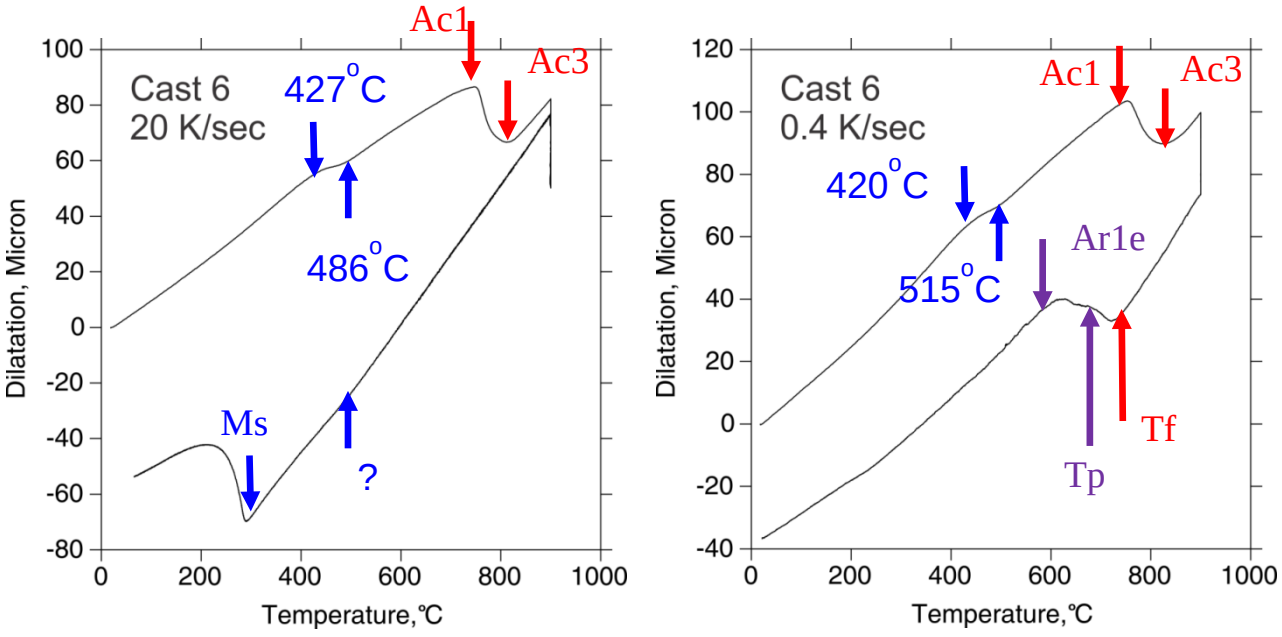

a) Cooling rate 20K/s **b) Cooling rate 0.4K/s**

Figure 12. Dilatometry measurements of alloy 6 at different cooling rates.

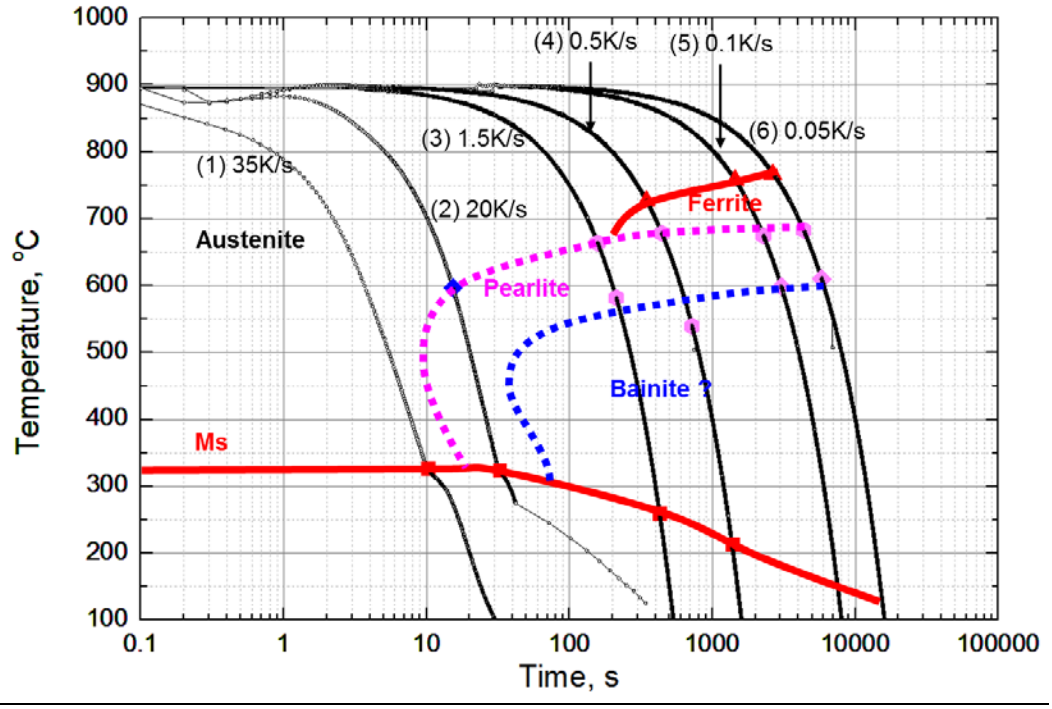

Figure 13. CCT diagram of alloy 6 constructed based on dilatometry measurements at different cooling rates

Effect of Temper Treatment

Literature indicated that temper could promote isothermal transformation from retained austenite to bainite and hence increase strength and toughness. To explore such feasibility, the samples from keel blocks cast at SCP were normalized with still-air or fan cooling, followed by temper treatment at 225°C or 500°C.

Alloy 1

Tensile test results for an alloy 1 sample from a 3" mid-radius bar were 748 MPa UTS, 420 MPa YS, and 5.8% elongation. Its yield strength was quite far below the goal of 615 MPa due to its low carbon content. It was less likely to have significant improvements in strength, and thus no temper was carried out for this alloy.

Alloy 2

Figure 14 shows the effects of temper on the strength and elongation of alloy 2. In comparison to properties without temper (UTS: 798-806 MPa, YS: 503-509 MPa, elongation: 8.6-10.6%), temper at 225°C had relatively weak effect. However, temper at 500°C showed a very strong effect. It caused a slight decrease of UTS, but certain increase of YS and significant increase of elongation. The effect of fan cooling was more evident on UTS and YS. These results are presented in Figure 15 together with results for samples with no temper for comparison. Table 5 details the alloy 2 heat treatments. Despite improvements from temper at 500°C, the YS after temper was still below the goal. Microstructures are presented in Figure 16 for SCP keel block samples after different heat treatments. A preliminary analysis indicated that the white areas are ferrite, dark areas adjacent to white areas are pearlite, and brown

areas are a mixture with martensite and bainite, see Figure 17. More detailed microstructure characterization is in order.

Alloy 3

Tensile test results for alloy 3 after temper are presented in Figure 18, which show similar temper effects on strength and elongation as alloy 2 because their compositions are quite similar to each other. Figure 19 shows a comparison of the samples with and without temper treatment. Table 6 details the alloy 3 heat treatments. Samples after temper at 500°C were very close to meeting the material strength goals (UTS>850 MPa, YS>615 MPa, elongation>10%). Figure 20 shows microstructures of SCP keel block samples after different heat treatments.

Alloy 4

Eight different heat treatments were carried out for alloy 4 by choosing different solution temperatures and times, and tensile test results are presented in Figure 21. This alloy also showed a strong effect from temper at 500°C; there was small variation of UTS, certain increase of YS, and significant increase of elongation. From Figure 21 it was observed that higher solution temperatures gave rise to higher elongation without sacrificing UTS and YS relative to lower solution temperatures. Those results are summarized in Figure 22 including a comparison to with no temper treatment. Table 7 details the alloy 4 heat treatments. Since alloy 4 had slightly higher carbon, its strength (UTS and YS) after temper at 500°C was higher than alloy 3 and both strength and elongation met the goals. Microstructure is presented in Figure 23 for SCP keel block samples after different heat treatments.

Alloy 5

No test samples were cast.

Alloy 6

Similar to alloy 4, there were also eight different heat treatments carried out for alloy 6 and tensile test results are presented in Figure 24. Again, the most significant improvement in elongation was due to temper at 500°C, which also resulted in increases of both UTS and YS relative to the samples without temper. From Figure 24 it was again observed that higher solution temperatures were better for UTS and YS, and together with fan-cooling led to even higher yield strengths. Figure 25 shows those results in comparison to samples with no temper. Table 8 details the alloy 6 heat treatments. The samples after temper at 500°C easily met the strength and elongation goals. Figure 26 shows the microstructures of SCP keel block samples after different heat treatments.

Alloy 7

There were only test bar samples of alloy 7 cast at STL, and tensile test after normalization at 960°C for 3 hours showed ~750 MPa UTS, ~510 MPa YS, and 2-3% elongation. No temper treatment was carried out for this alloy.

Alloy 8 (with boron)

Tensile test results for alloy 8 under the eight different heat treatment conditions also used for alloys 4 and 6 are presented in Figure 27. For this alloy, the effects of temper at 500°C led not only to significant improvements in elongation, but also considerable increases in UTS and YS. It was observed that the higher solution temperature led to more improvement in elongation. Figure 28 shows a comparison of alloy 8 samples with and without a temper treatment. The first three samples were from the first two heats and had four times the boron concentration of all the other samples. Table 9 details the alloy 8 heat treatments. The samples treated at the higher solution temperatures and higher temper

temperature met the material strength and elongation goals. Foundry practice has shown that it is difficult to control the boron content during melting, which would be a challenge in a production environment. Figure 30 shows the microstructures of SCP keel block samples after different heat treatments.

Alloy 9
No test samples were cast.

Alloy 10 and 11
Each of these two alloys were given seven different heat treatments including water quenching, temper, and furnace holding. The tensile test results are presented in Figure 31 and Table 10 details the heat treatments. It was observed that both alloys treated by normalization and 500^{o}C temper met the strength and elongation goals. The importance of the 500^{o}C temper for these alloys is evident when the results of samples 5 and 7 are compared to sample 6. The homogenization step is not necessary. Despite the impressive strength and elongation of the sample 6 heat treatments on alloys 10 and 11, these two alloys probably don't have sufficient hardenability for induction hardening due to their low carbon concentrations.

Alloy 12, 13, and 14
The yield strengths of alloys 12 and 13 were far below the goal of 615 MPa as can be observed in Figure 32. No temper treatment was carried out for these two alloys.

Figure 33 shows tensile test results for alloy 14 under the various heat treatment conditions listed in Table 11. It was observed that temper at 500^{o}C or 649^{o}C led to large improvements in elongation, but left the yield strengths well below the goal.

Comparison of all alloys
Figure 34 shows tensile test results of all samples tempered at 225^{o}C and it was observed that none of the alloys with this temper treatment are capable of meeting the goals due to either low YS and/or low elongation. The most favorable tensile test results of samples from each alloy are presented in Figure 35. It was concluded that alloys 3, 4, 6, 8, 10, and 11 with a normalization and 500^{o}C temper treatment could meet the strength and elongation goals, while alloys 2, 12, 13, and 14 as heat treated for these studies could not meet the goals.

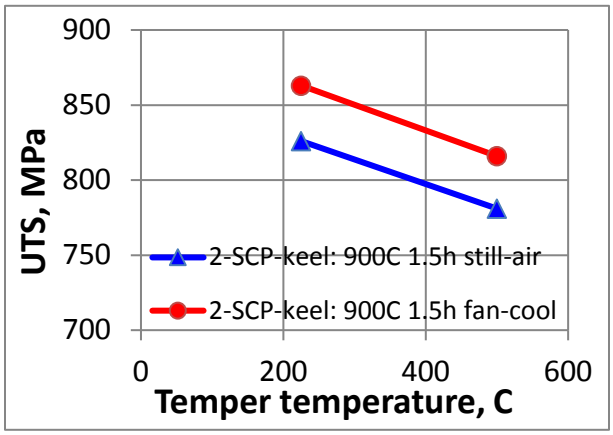

a) Temper effect on UTS

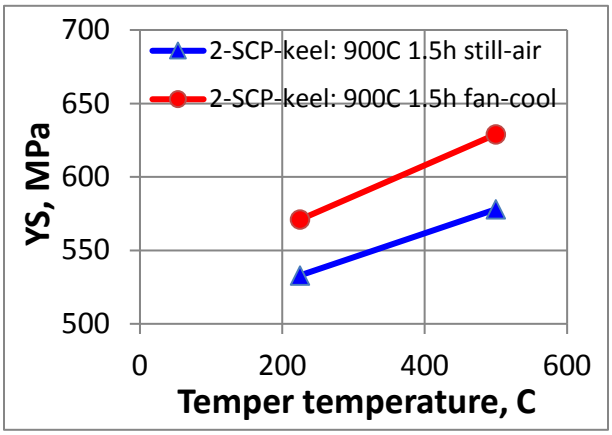

b) Temper effect on YS

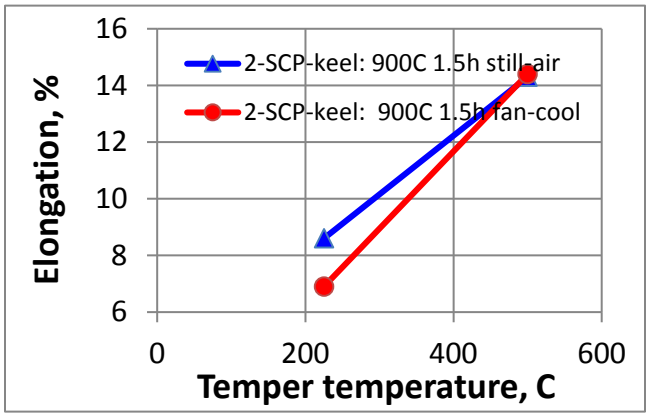

c) Temper effect on elongation

Figure 14. Effect of temper treatment on mechanical properties of alloy 2

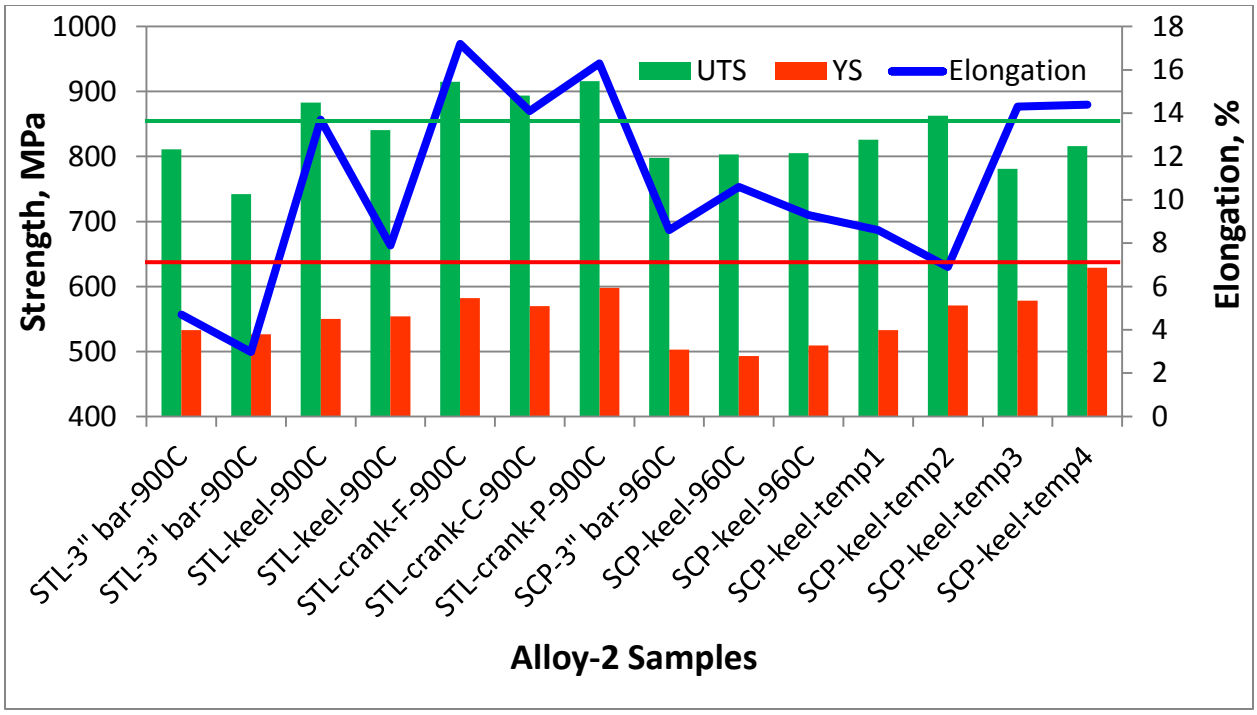

Figure 15. Tensile test results of alloy 2 after treatment as shown in the following table

Table 5. Heat treatments for alloy 2

Notation	Heat treatment	Temper
1st 10 samples	900°C or 960°C 3h still-air	No
Temp1	900°C 1.5h still-air	225°C 2h
Temp2	900°C 1.5h fan-cool	225°C 2h
Temp3	900°C 1.5h still-air	500°C 4h
Temp4	900°C 1.5h fan-cool	500°C 4h

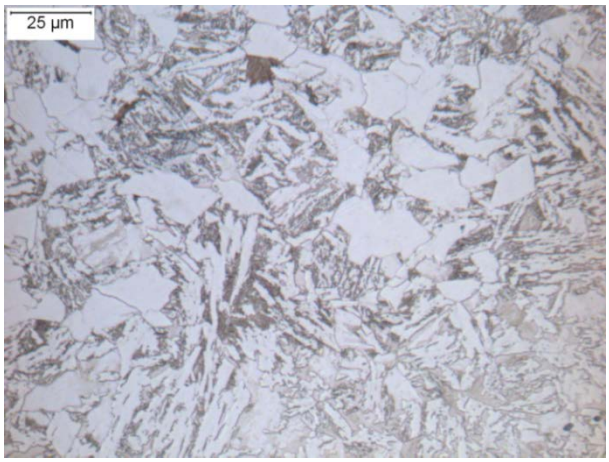

a) 960°C 3hr →still-air

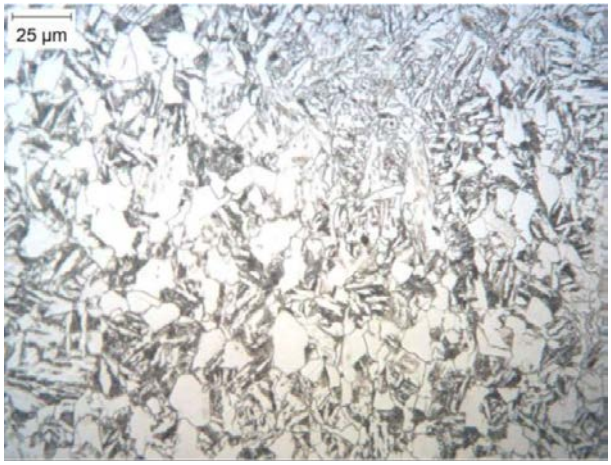

b) 900°C 1.5hr → still-air → 225°C 2hr

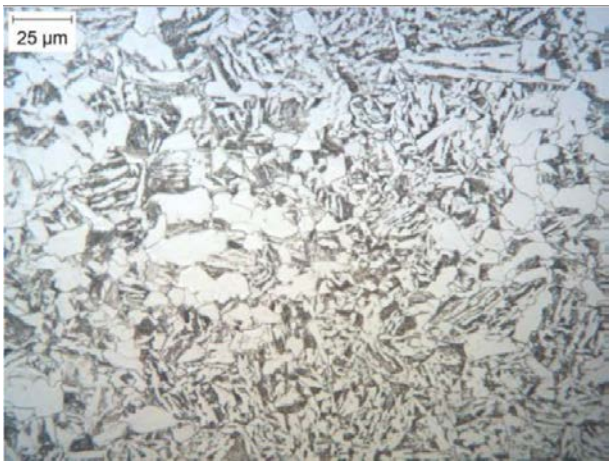

c) 900°C 1.5hr → still-air → 550°C 4hr

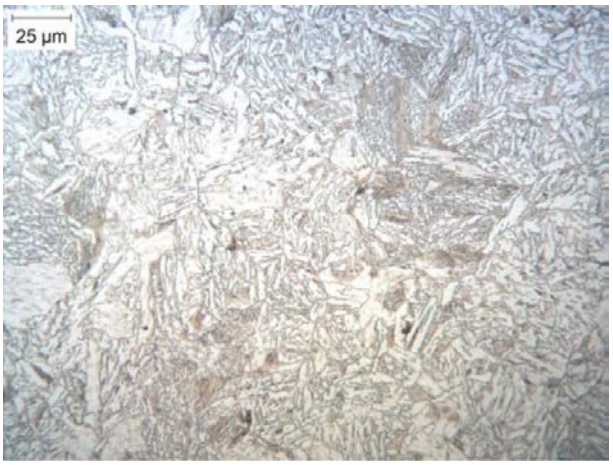

d) 900°C 1.5hr → fan-cool → 225°C 2hr

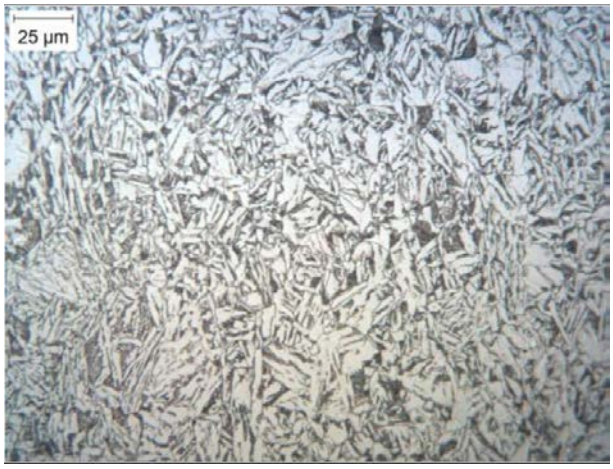

e) 900°C 1.5hr → fan-cool → 550°C 4hr

Figure 16. Microstructure of alloy 2 SCP keel block samples after different treatments. White area is ferrite, dark area adjacent to white area is pearlite, and brown area is a mixture with martensite and bainite. [2% Nital 500x]

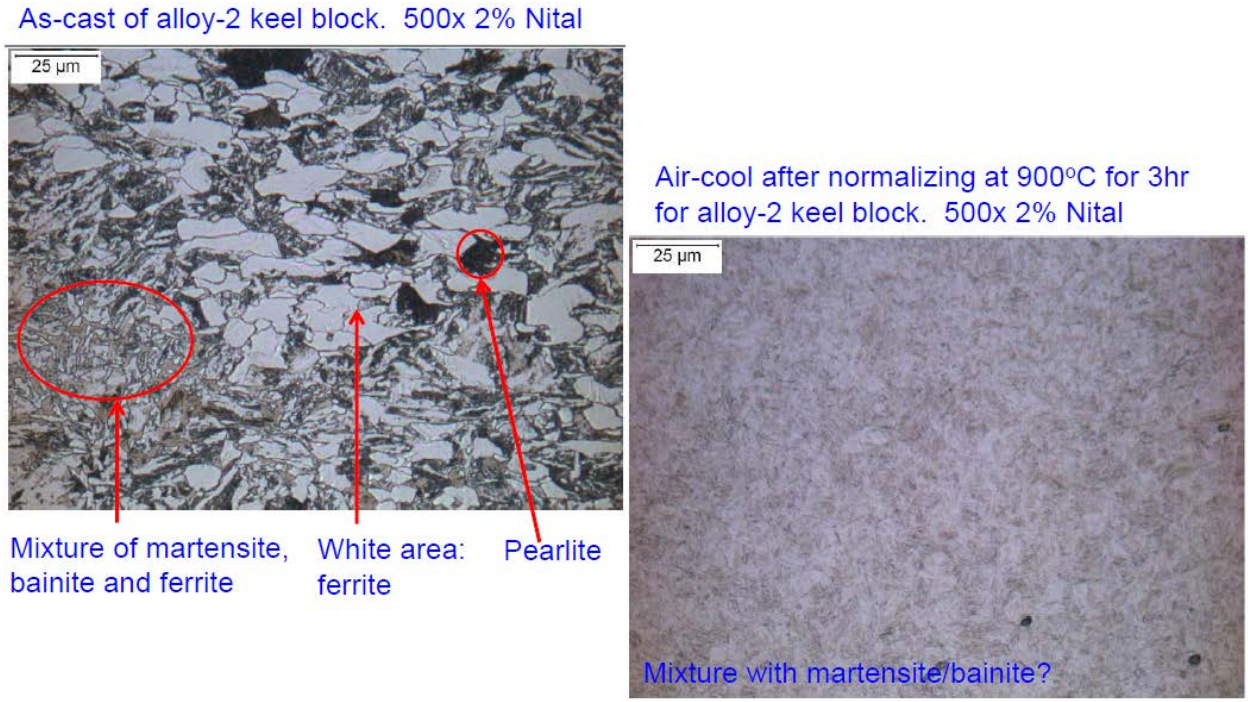

Figure 17. Microstructures from an alloy 2 keel block warrant further characterization, as do the microstructures from most of the alloys studied [2% Nital 500x]

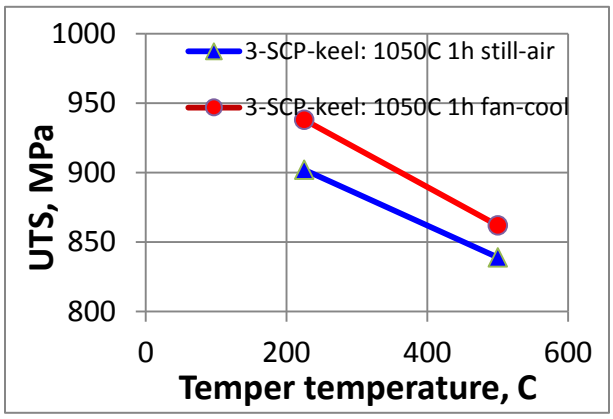

a) Temper effect on UTS

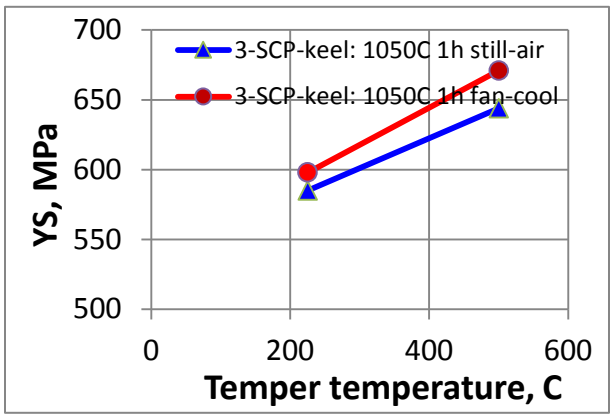

b) Temper effect on YS

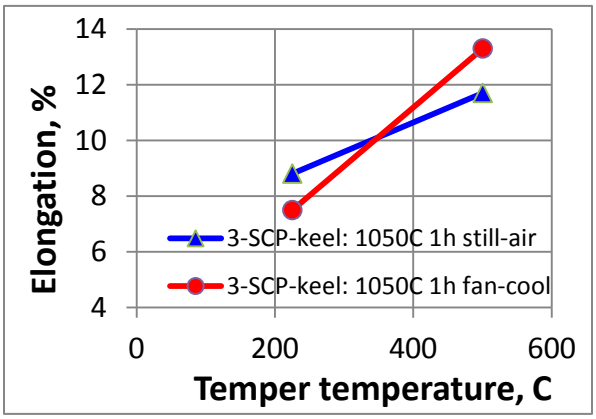

c) Temper effect on elongation

Figure 18. Effect of temper treatment on mechanical properties of alloy 3

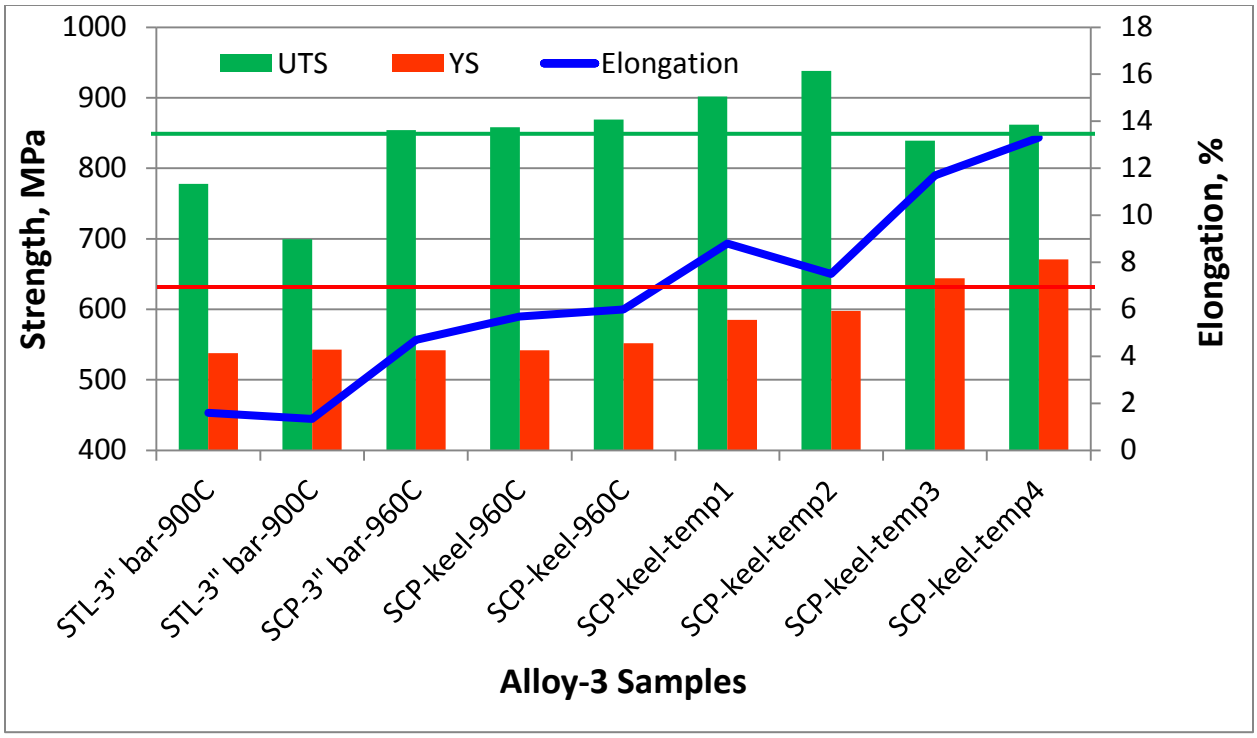

Figure 19. Tensile test results of alloy 3 after treatment as shown in the following table

Table 6. Heat treatments for alloy 3

Notation	Heat treatment	Temper
1st 5 samples	900°C or 960°C 3h still-air	No
Temp1	1050°C 1h still-air	225°C 2h
Temp2	1050°C 1h fan-cool	225°C 2h
Temp3	1050°C 1h still-air	500°C 4h
Temp4	1050°C 1h fan-cool	500°C 4h

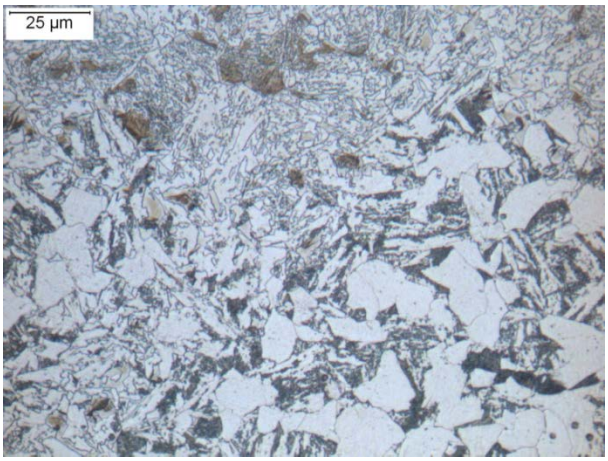

a) 960°C 3hr →still-air

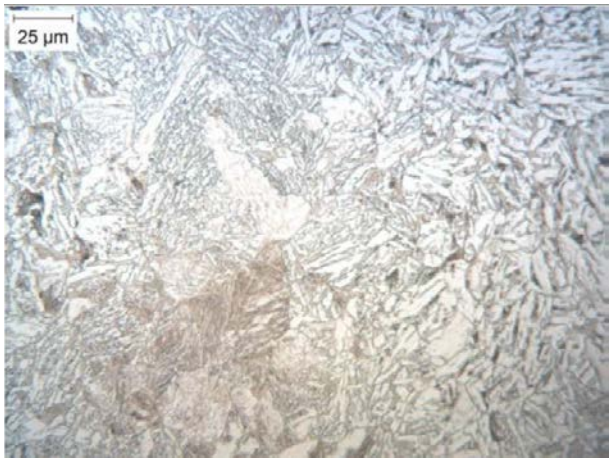

b) 1050°C 1hr → still-air → 225°C 2hr

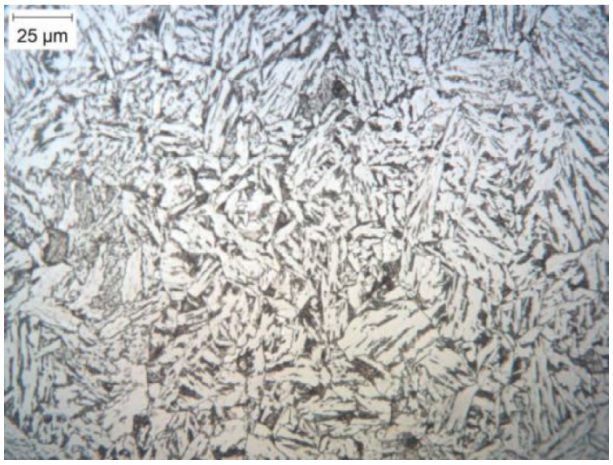

c) 1050°C 1hr → still-air → 550°C 4hr

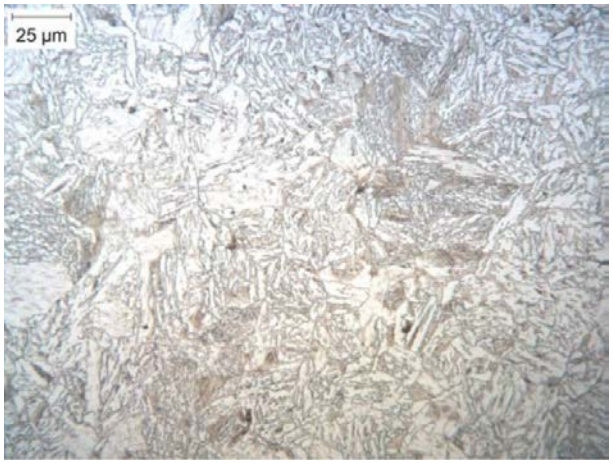

d) 1050°C 1hr → fan-cool → 225°C 2hr

e) 1050°C 1hr → fan-cool → 550°C 4hr

Figure 20. Microstructure of alloy 3 SCP keel block samples after different treatments. White area is ferrite, dark area adjacent to white area is pearlite, and brown area is a mixture with martensite and bainite. [2% Nital 500x]

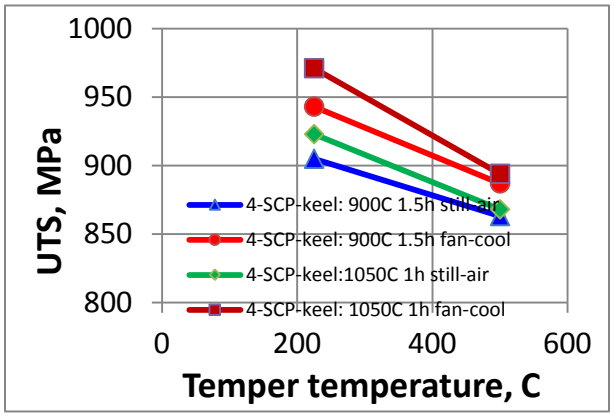

a) Temper effect on UTS

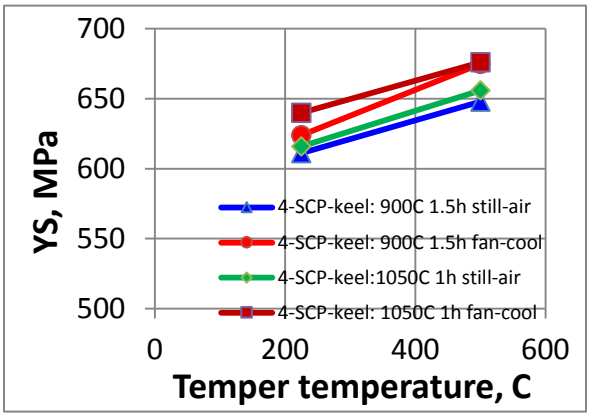

b) Temper effect on YS

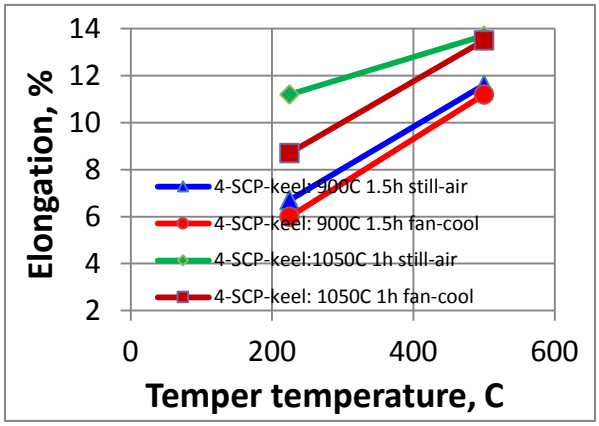

c) Temper effect on elongation

Figure 21. Effect of temper treatment on mechanical properties of alloy 4

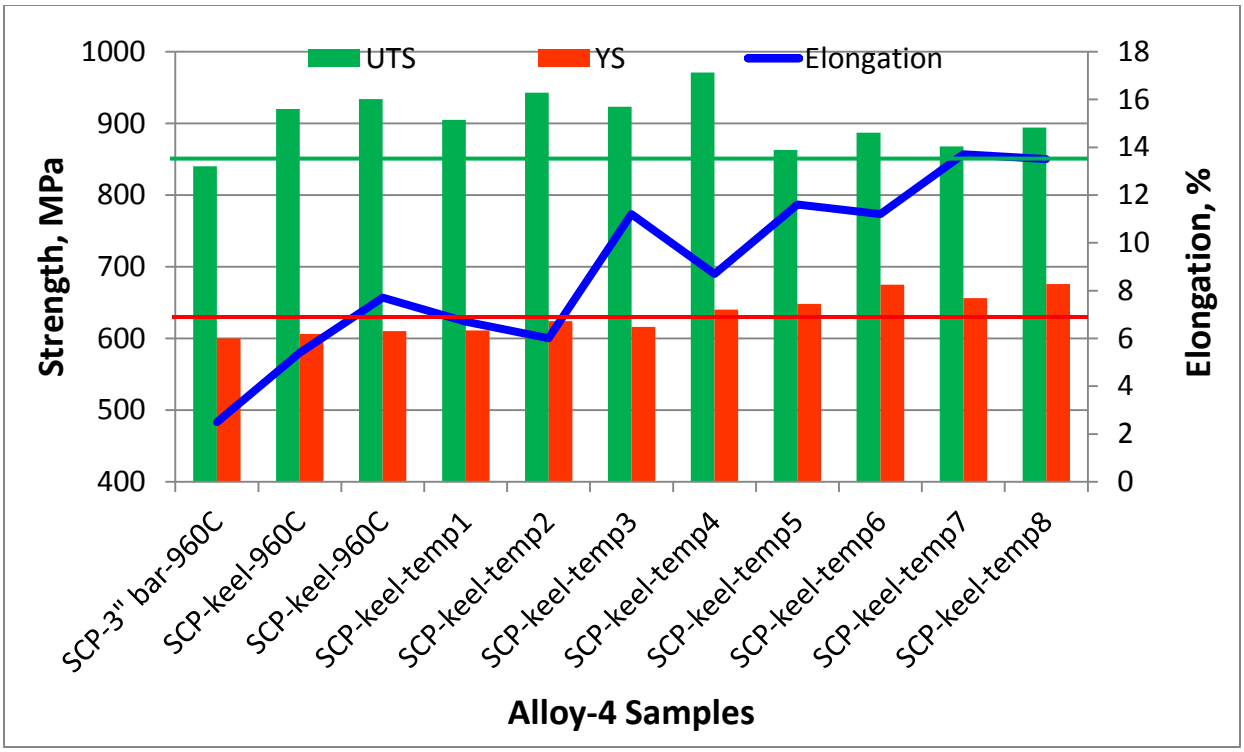

Figure 22. Tensile test results of alloy 4 after treatment as shown in the following table

Table 7. Heat treatments for alloy 4

Notation	Heat treatment	Temper
1st 3 samples	960°C 3h still-air	No
Temp1	900°C 1.5h still-air	225°C 2h
Temp2	900°C 1.5h fan-cool	225°C 2h
Temp3	1050°C 1h still-air	225°C 2h
Temp4	1050°C 1h fan-cool	225°C 2h
Temp5	900°C 1.5h still-air	500°C 4h
Temp6	900°C 1.5h fan-cool	500°C 4h
Temp7	1050°C 1h still-air	500°C 4h
Temp8	1050°C 1h fan-cool	500°C 4h

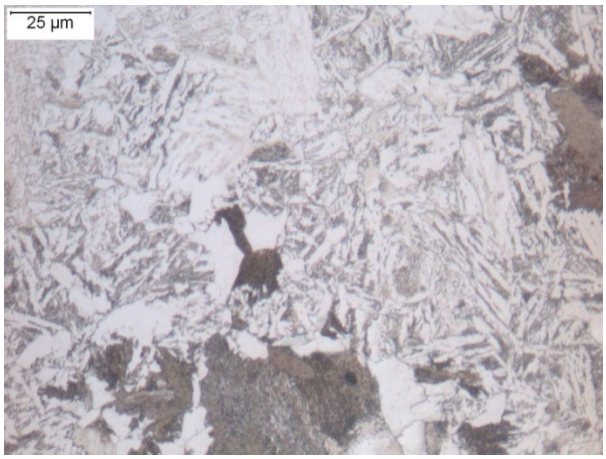

a) 960°C 3hr →still-air

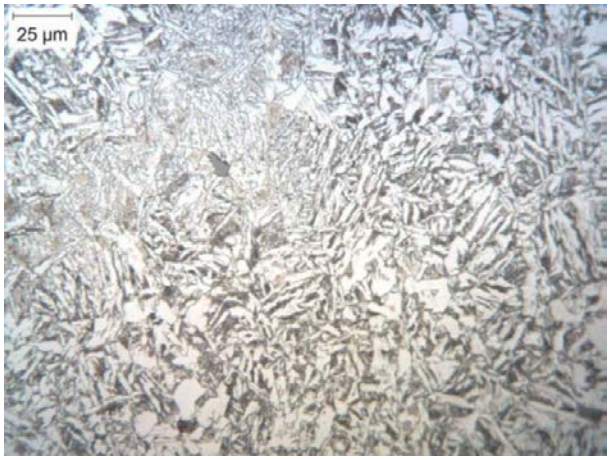

b) 900°C 1.5hr → still-air → 225°C 2hr

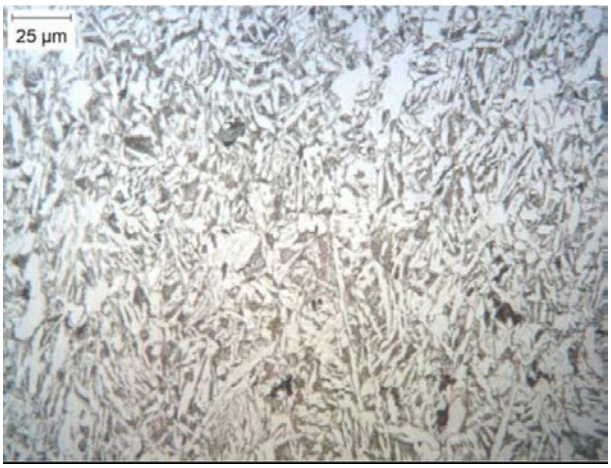

c) 900°C 1.5hr → still-air → 550°C 4hr

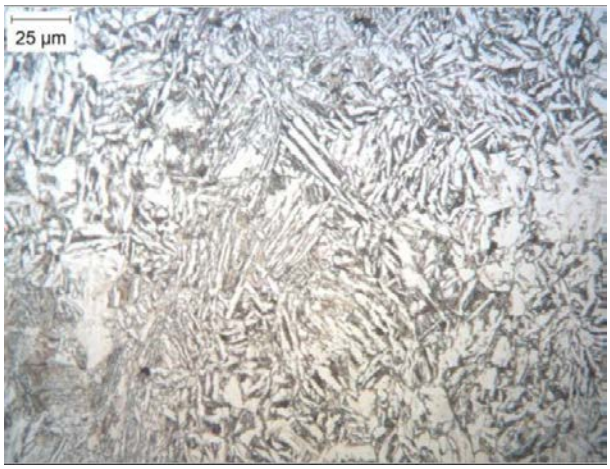

d) 1050°C 1hr → still-cool → 225°C 2hr

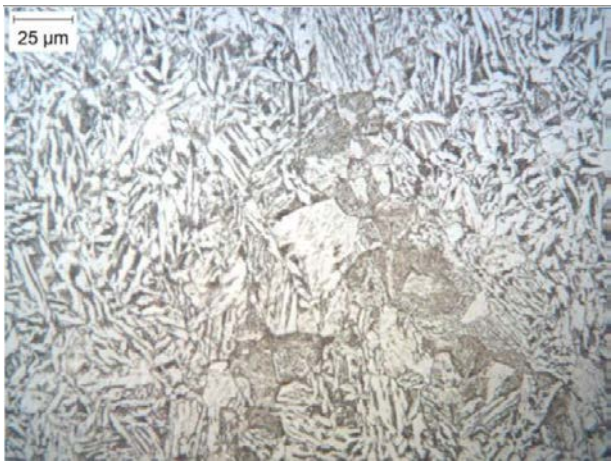

e) 900°C 1.5hr → still-air → 550°C 4hr

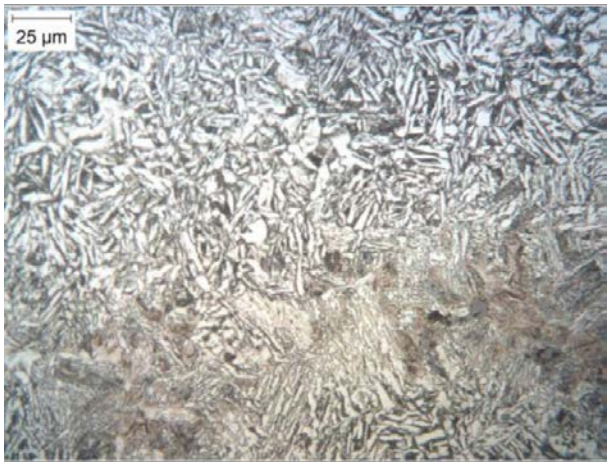

f) 900°C 1.5hr → fan-cool → 225°C 2hr

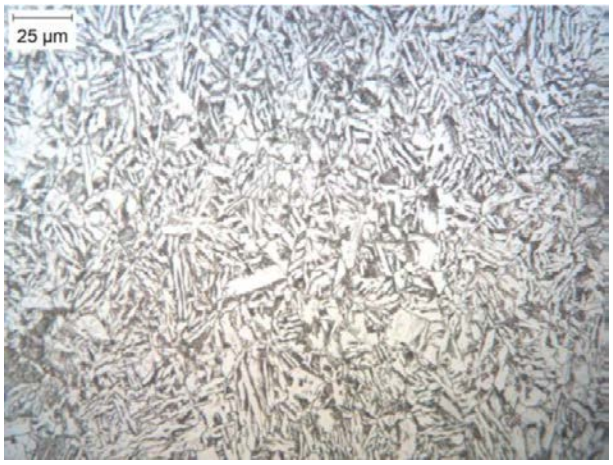

g) 900°C 1.5hr → fan-cool → 550°C 4hr

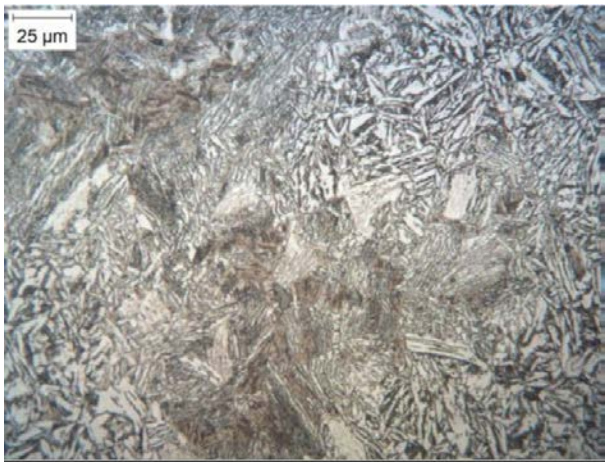

h) 1050°C 1hr → fan-cool → 225°C 2hr

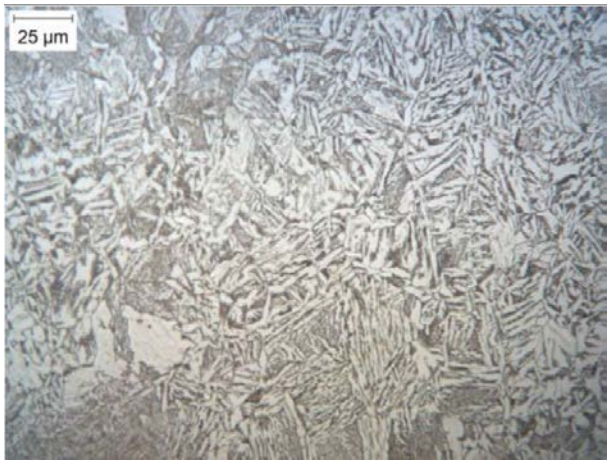

i) 1050°C 1hr → fan-air → 550°C 4hr

Figure 23. Microstructure of alloy 4 SCP keel block samples after different treatments. White area is ferrite, dark area adjacent to white area is pearlite, and brown area is a mixture with martensite and bainite. [2% Nital 500x]

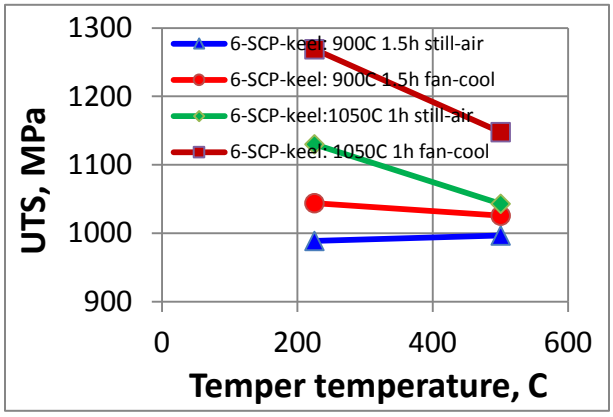

a) Temper effect on UTS

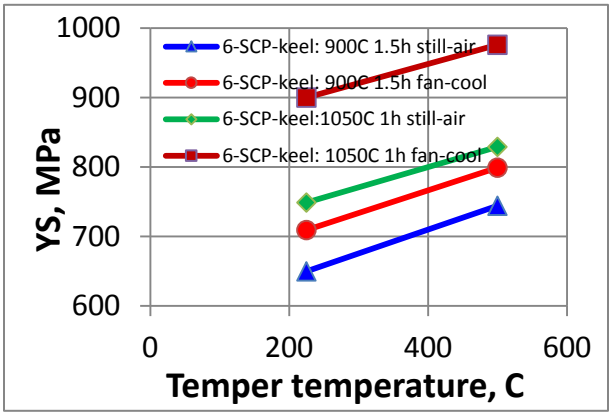

b) Temper effect on YS

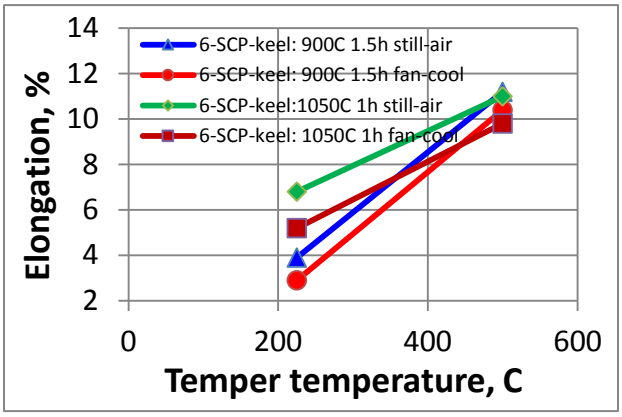

c) Temper effect on elongation

Figure 24. Effect of temper treatment on mechanical properties of alloy 6

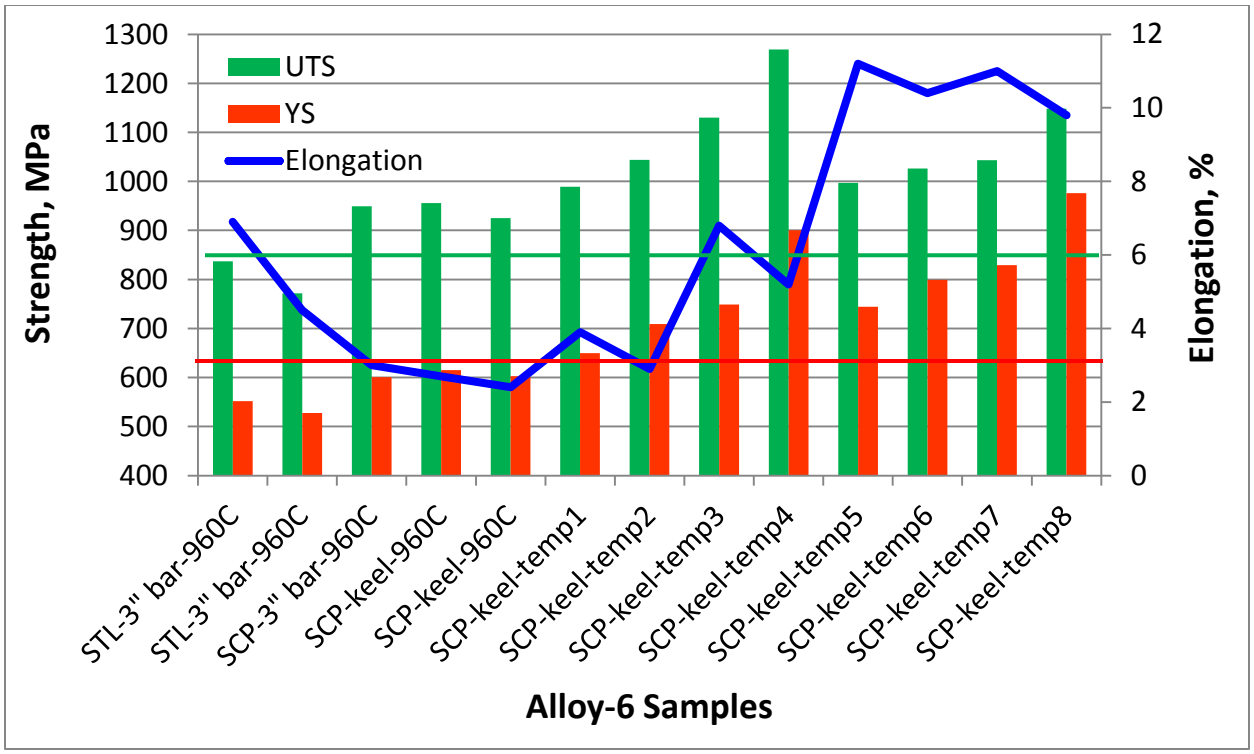

Figure 25. Tensile test results of alloy 6 after treatment as shown in the following table

Table 8. Heat treatments for alloy 6

Notation	Heat treatment	Temper
1st 3 samples	960°C 3h still-air	No
4th & 5th samples	960°C 1.5 still-air	No
Temp1	900°C 1.5h still-air	225°C 2h
Temp2	900°C 1.5h fan-cool	225°C 2h
Temp3	1050°C 1h still-air	225°C 2h
Temp4	1050°C 1h fan-cool	225°C 2h
Temp5	900°C 1.5h still-air	500°C 4h
Temp6	900°C 1.5h fan-cool	500°C 4h
Temp7	1050°C 1h still-air	500°C 4h
Temp8	1050°C 1h fan-cool	500°C 4h

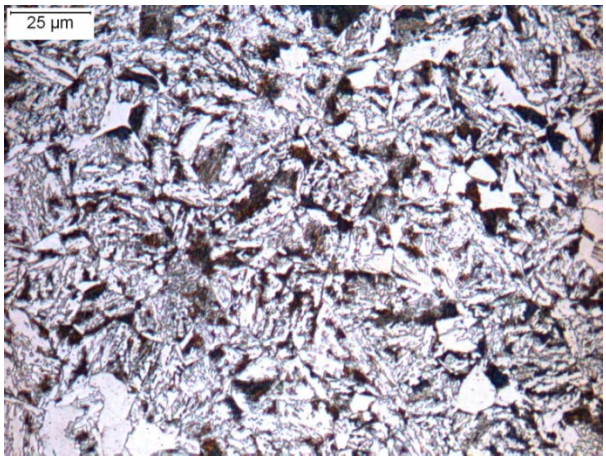

a) 960°C 3hr →still-air

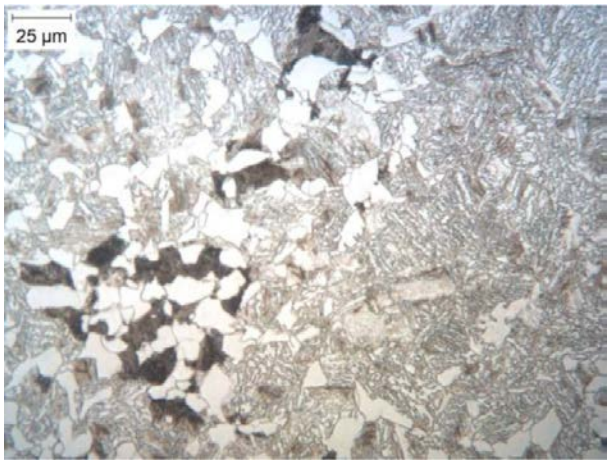

b) 900°C 1.5hr → still-air → 225°C 2hr

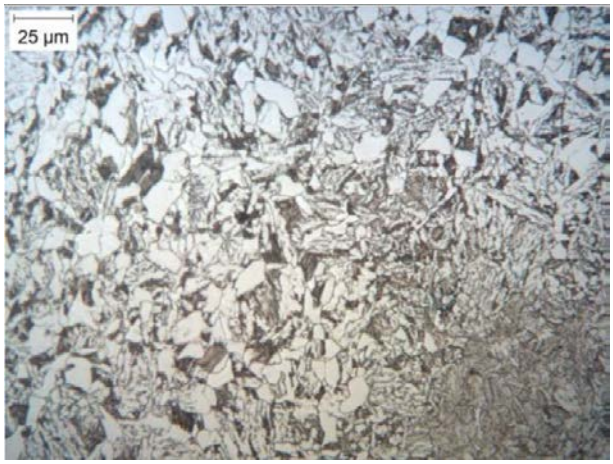

c) 900°C 1.5hr → still-air → 550°C 4hr

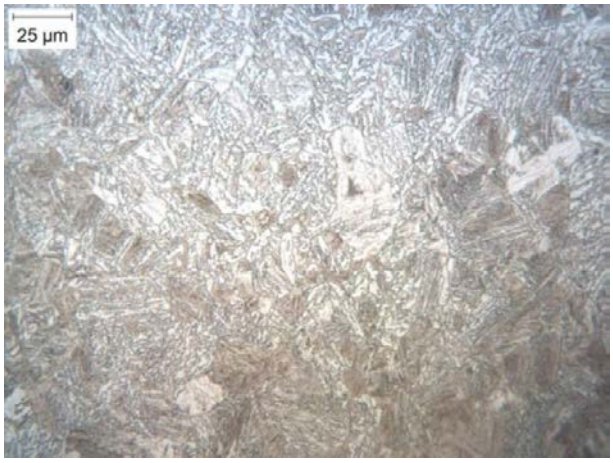

d) 1050°C 1hr → still-cool → 225°C 2hr

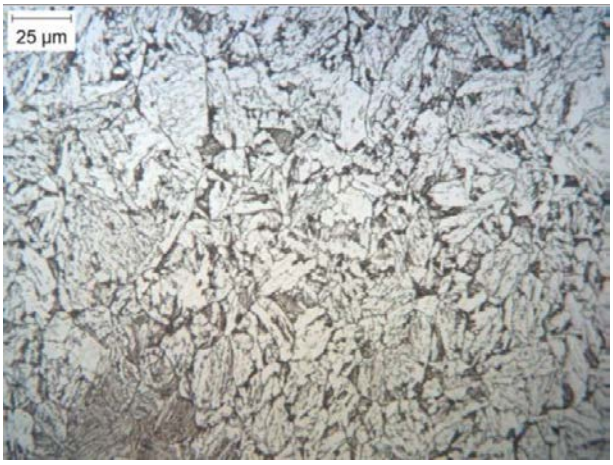

e) 900°C 1.5hr → still-air → 550°C 4hr

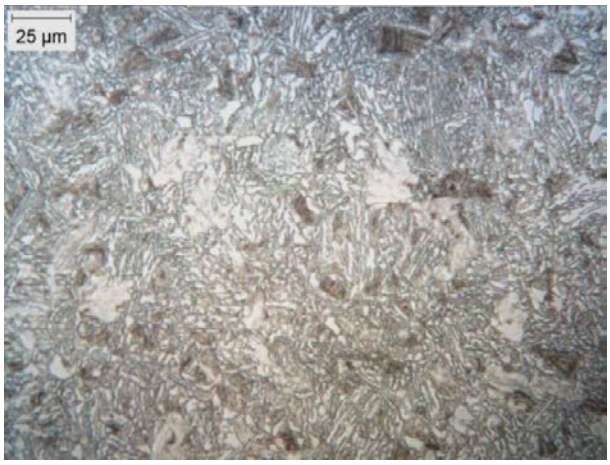

f) 900°C 1.5hr → fan-cool → 225°C 2hr

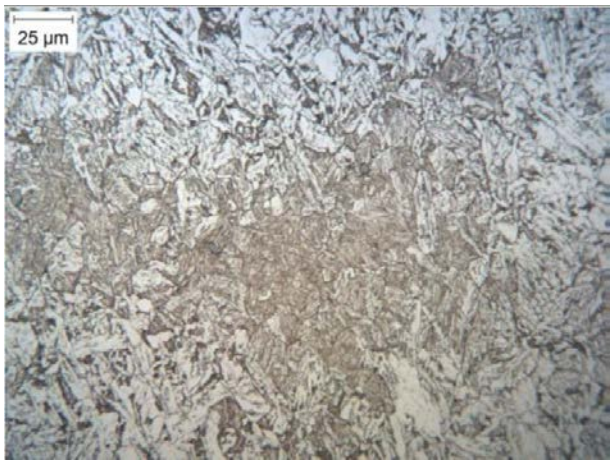

g) 900°C 1.5hr → fan-cool → 550°C 4hr

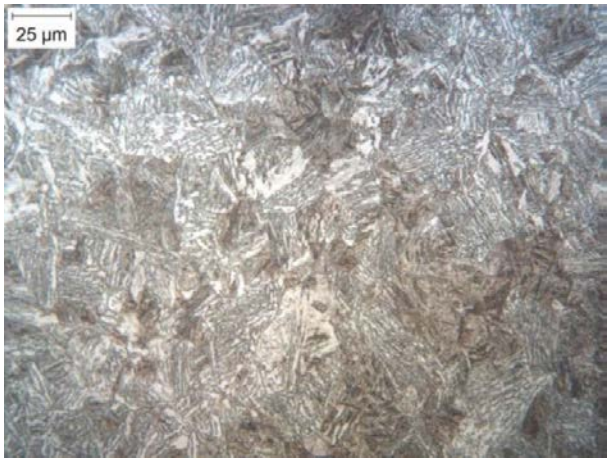

h) 1050°C 1hr → fan-cool → 225°C 2hr

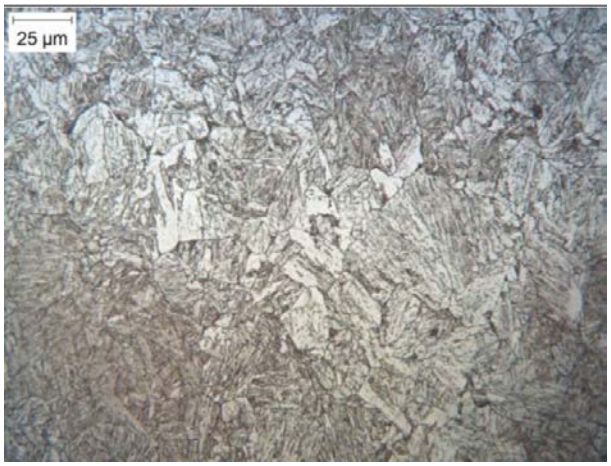

i) 1050°C 1hr → fan-air → 550°C 4hr

Figure 26. Microstructure of alloy 6 SCP keel block samples after different treatments. White area is ferrite, dark area adjacent to white area is pearlite, and brown area is a mixture with martensite and bainite. [2% Nital 500x]

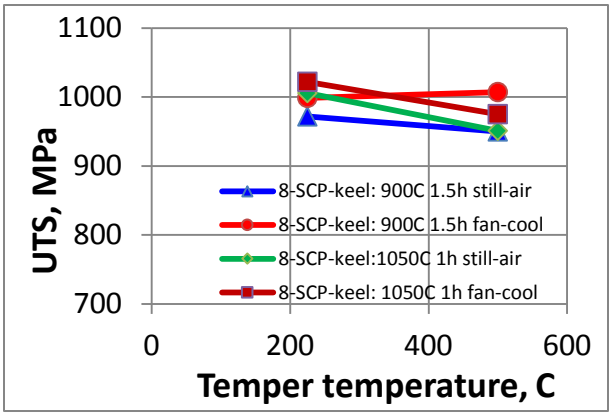

a) Temper effect on UTS

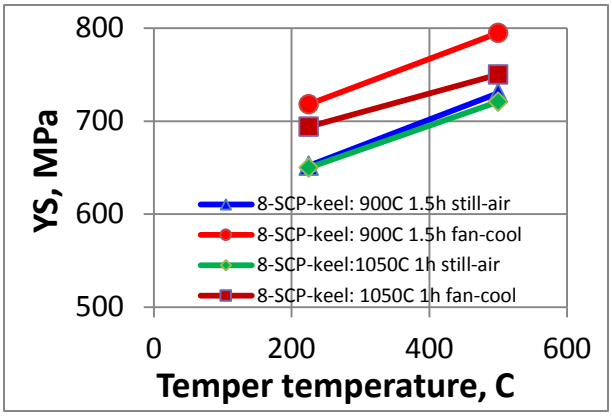

b) Temper effect on YS

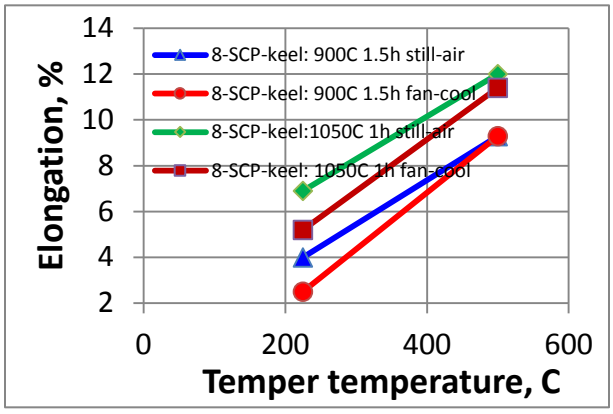

c) Temper effect on elongation

Figure 27. Effect of temper treatment on mechanical properties of alloy 8

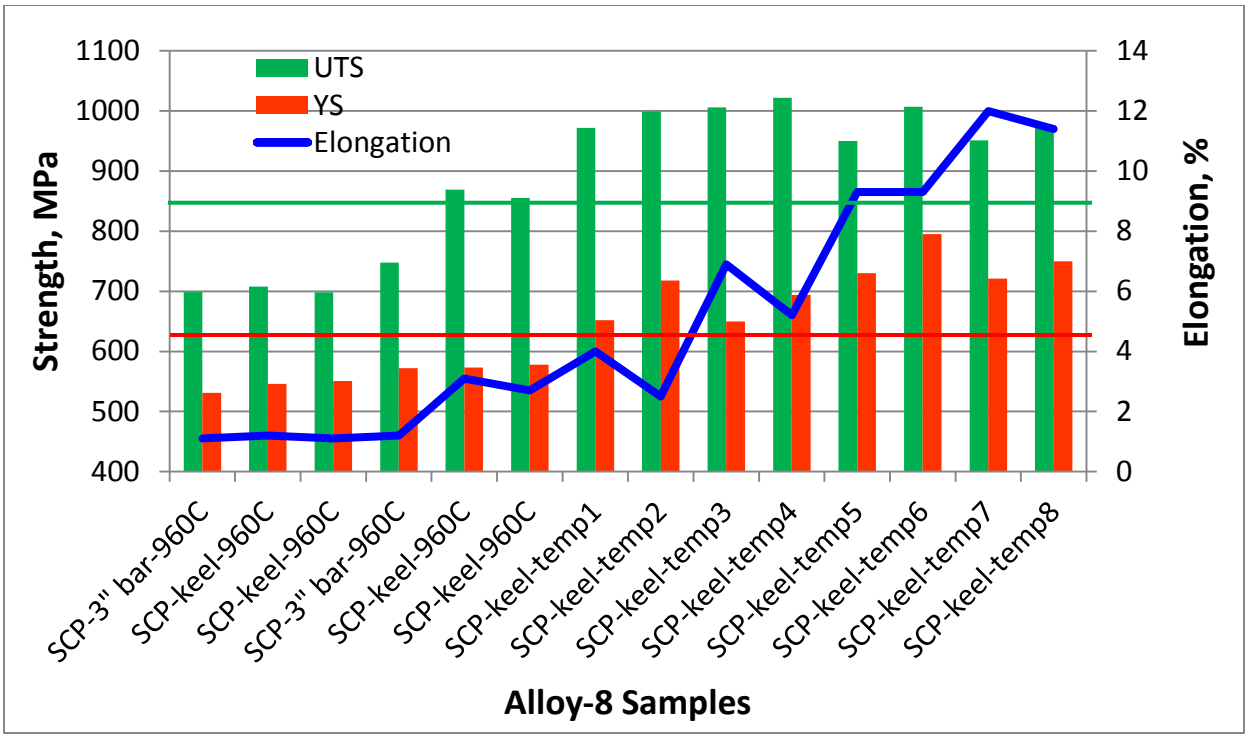

Figure 28. Tensile test results of alloy 8 after treatment as shown in the following table. The first 3 samples are from heat 1 with 4 times the boron of all other samples.

Table 9. Heat treatments for alloy-8

Notation	Heat treatment	Temper
1st 3 samples	960°C 3h still-air	No
2nd 3 samples	960°C 1.5 still-air	No
Temp1	900°C 1.5h still-air	225°C 2h
Temp2	900°C 1.5h fan-cool	225°C 2h
Temp3	1050°C 1h still-air	225°C 2h
Temp4	1050°C 1h fan-cool	225°C 2h
Temp5	900°C 1.5h still-air	500°C 4h
Temp6	900°C 1.5h fan-cool	500°C 4h
Temp7	1050°C 1h still-air	500°C 4h
Temp8	1050°C 1h fan-cool	500°C 4h

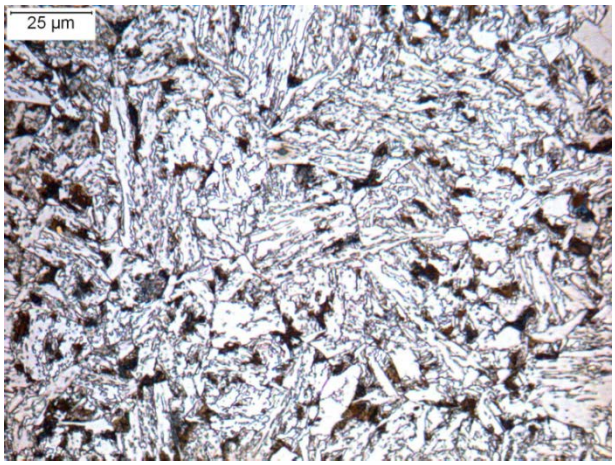

a) 960°C 3hr →still-air

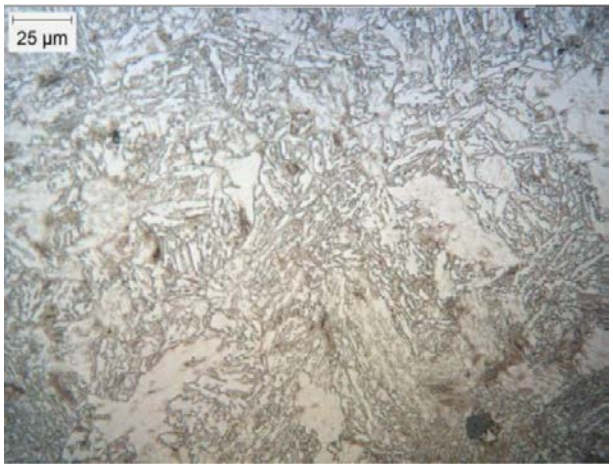

b) 900°C 1.5hr → still-air → 225°C 2hr

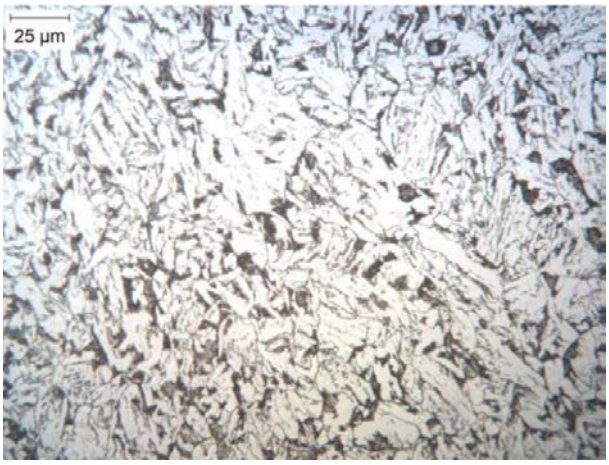

c) 900°C 1.5hr → still-air → 550°C 4hr

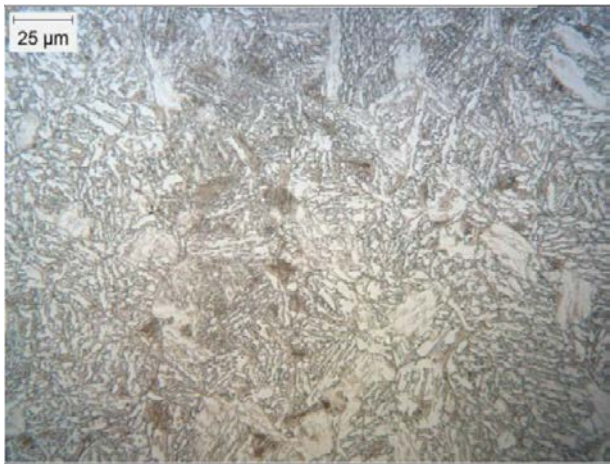

d) 1050°C 1hr → still-cool → 225°C 2hr

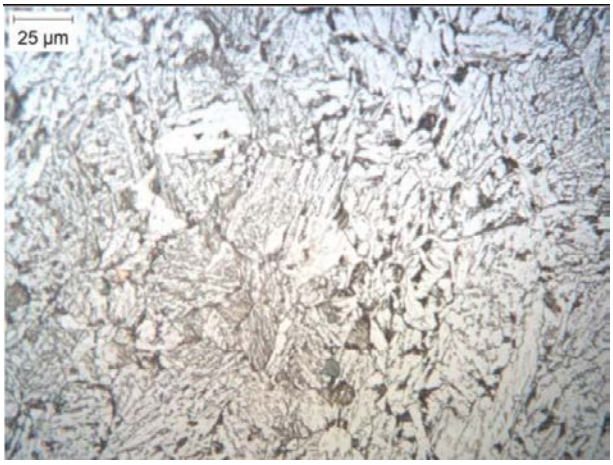

e) 900°C 1.5hr → still-air → 550°C 4hr

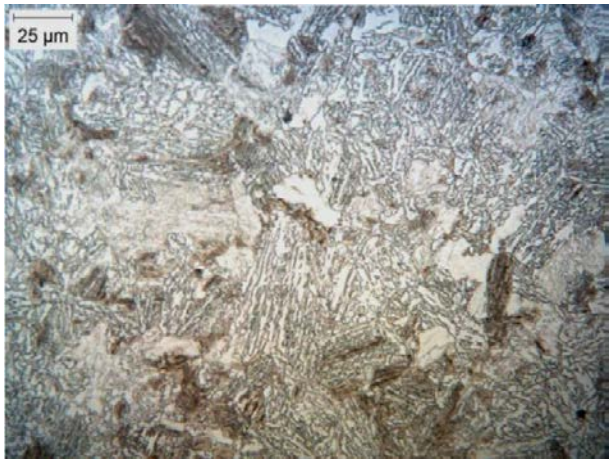

f) 900°C 1.5hr → fan-cool → 225°C 2hr

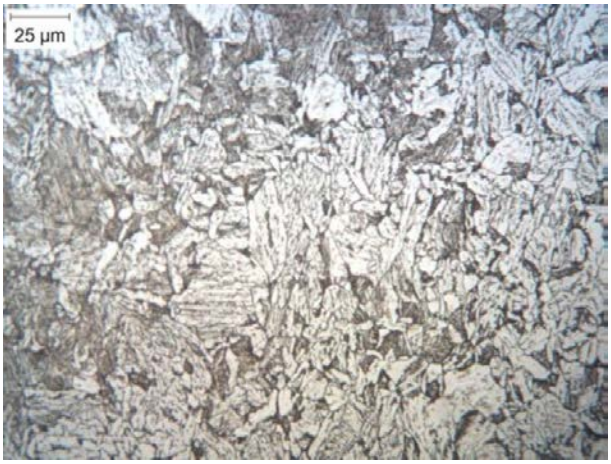

g) 900°C 1.5hr → fan-cool → 550°C 4hr

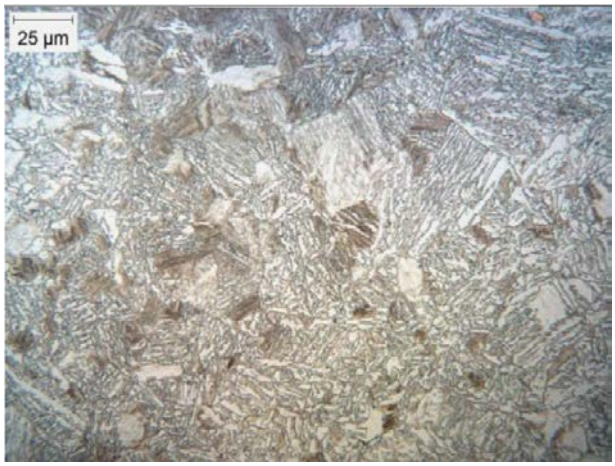

h) 1050°C 1hr → fan-cool → 225°C 2hr

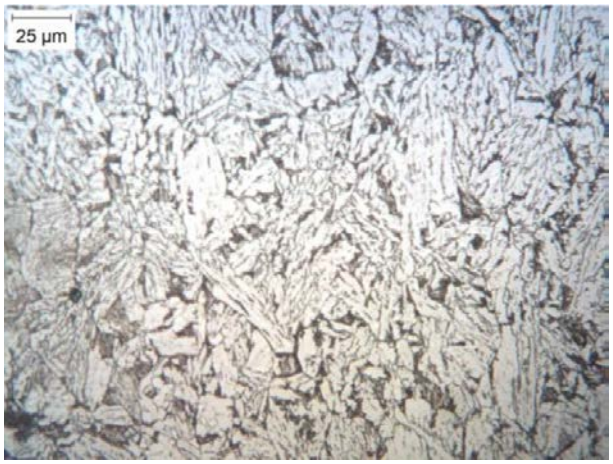

i) 1050°C 1hr → fan-air → 550°C 4hr

Figure 30. Microstructure of alloy 8.2 SCP keel block samples at the lower boron concentration after different treatments. White area is ferrite, dark area adjacent to white area is pearlite, and brown area is a mixture with martensite and bainite. [2% Nital 500x]

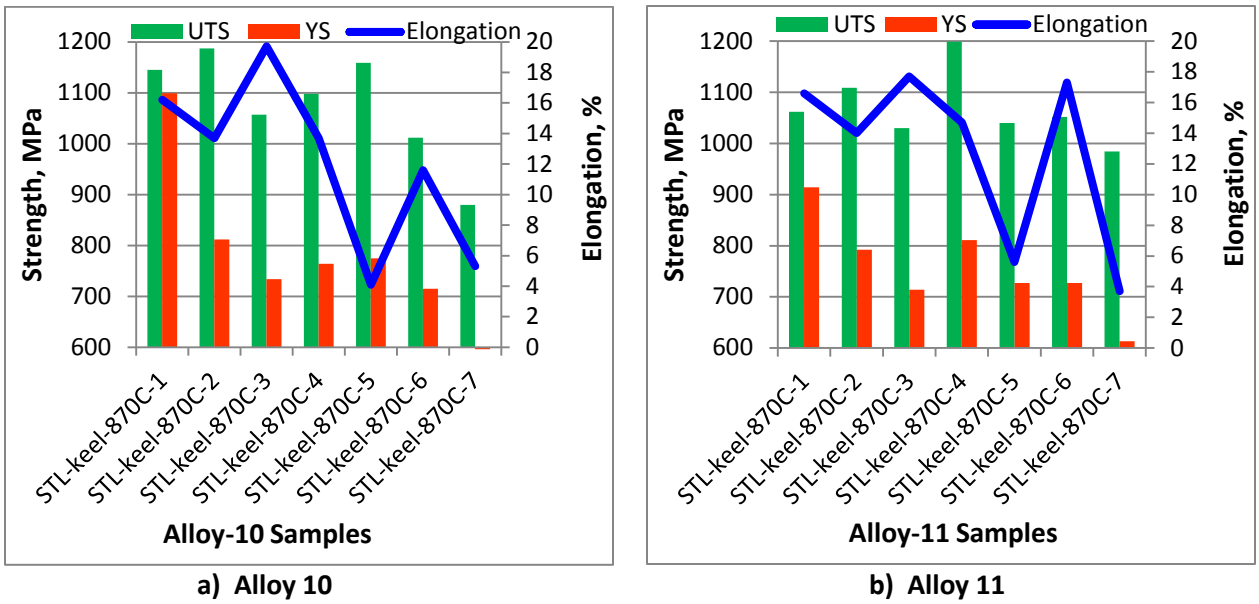

a) Alloy 10

b) Alloy 11

Figure 31. Tensile test results of alloys 10 and 11 after treatment as shown in the following table

Table 10. Heat treatments for alloys 10 and 11

Notation	Homogenization 1050°C 0.75h	Solution 870°C 1h	Furnace hold or Temper
Sample 1	water quench	water quench	500°C 4h
Sample 2	water quench	still-air to 500°C	Furnace 450°C 4h
Sample 3	still-air	still-air	500°C 4h
Sample 4	Still-air	still-air to 500°C	Furnace 450°C 4h
Sample 5	No	still-air to 500°C	Furnace 450°C 1h?
Sample 6	No	still-air	500°C 4h
Sample 7	No	2h still-air	No

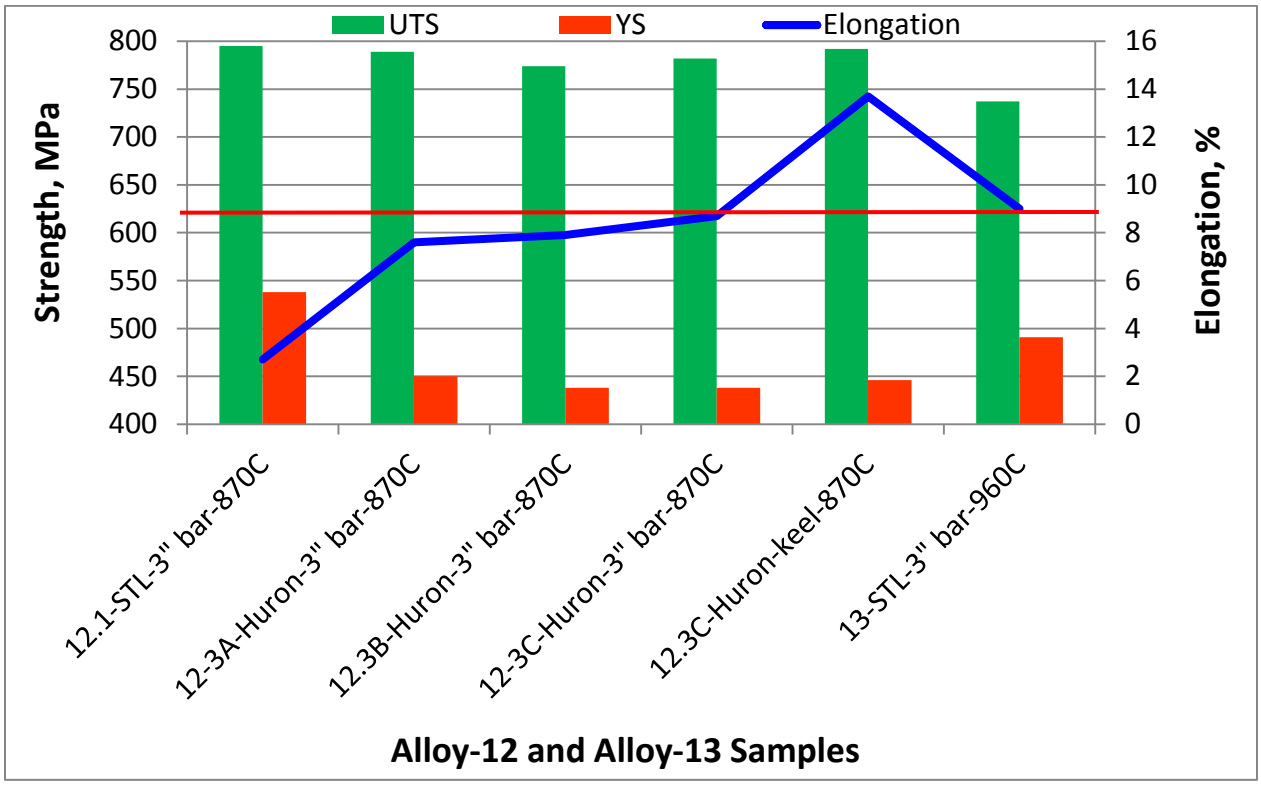

Figure 32. Tensile test results of alloy 12 after normalization at 870°C for 3 hours and alloy 13 after normalization at 960°C for 3 hours

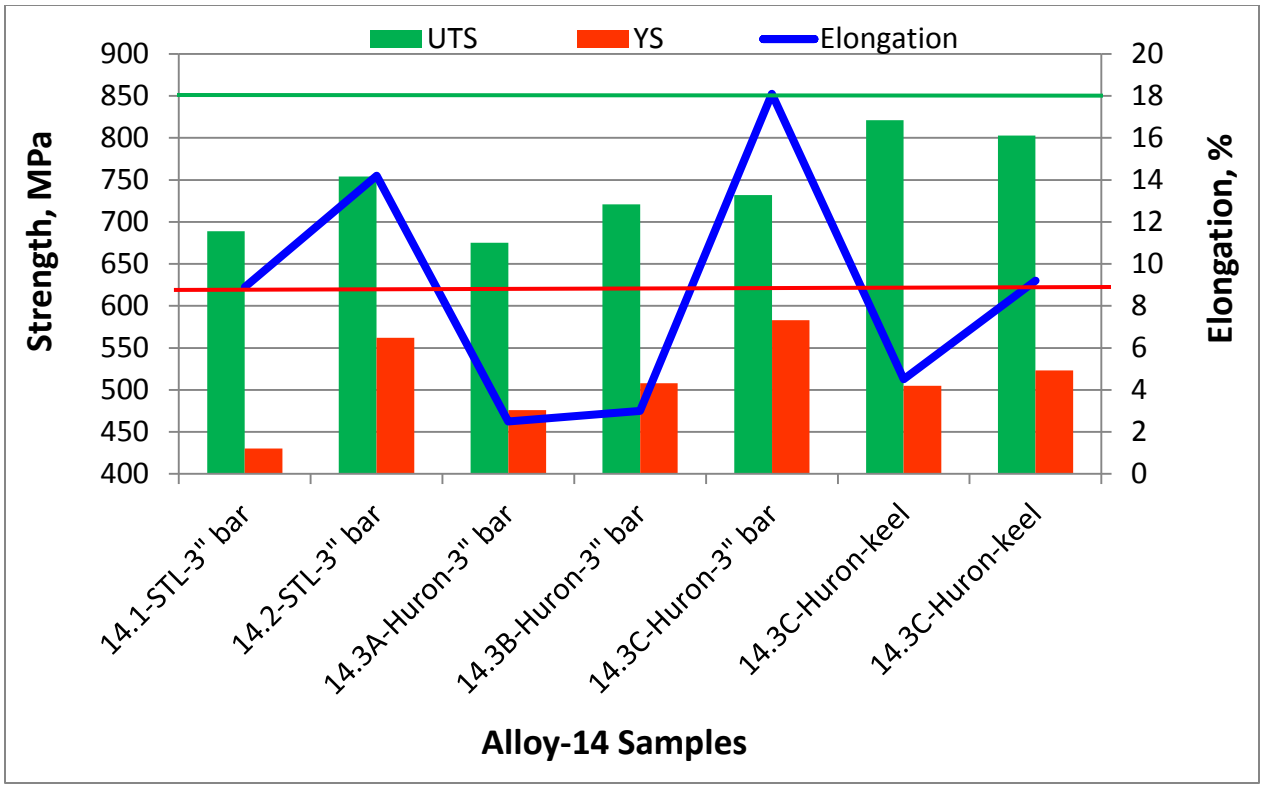

Figure 33. Test results of alloy 14 after treatment as shown in the following table

Table 11. Heat treatments for alloy 14

Notation	Homogenization	Solution	Temper
14.1 bar	No	960°C 3h Still-air	No
14.2 bar	860°C 3h Oil quench	960°C 3h Still-air	500°C 4h
14.3A bar	No	870°C 3h Still-air	No
14.3B bar	No	870°C 3h Still-air	No
14.3C-bar	899°C 3h water quench	No	649°C 2h
14.3C-keel	No	870°C 3h Still-air	No
14.3C-keel	No	870°C 3h Still-air	No

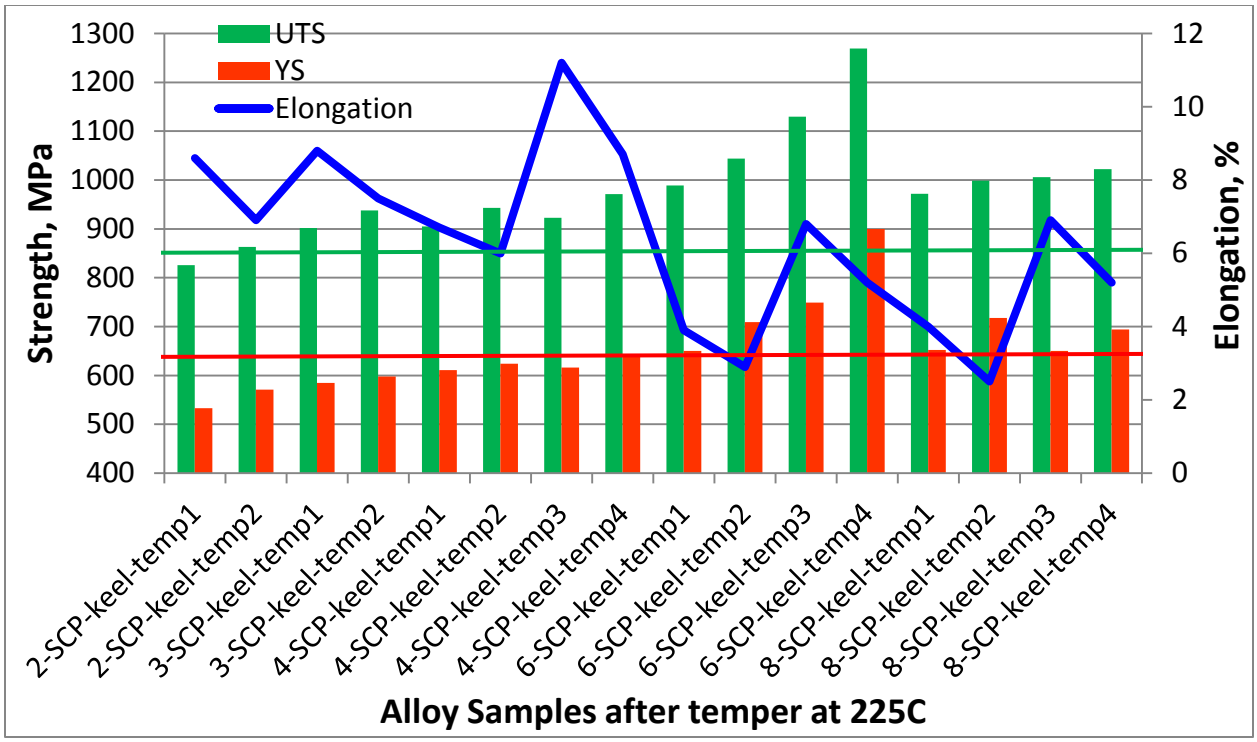

Figure 34. Tensile test results of alloy samples after normalization and temper at 225°C

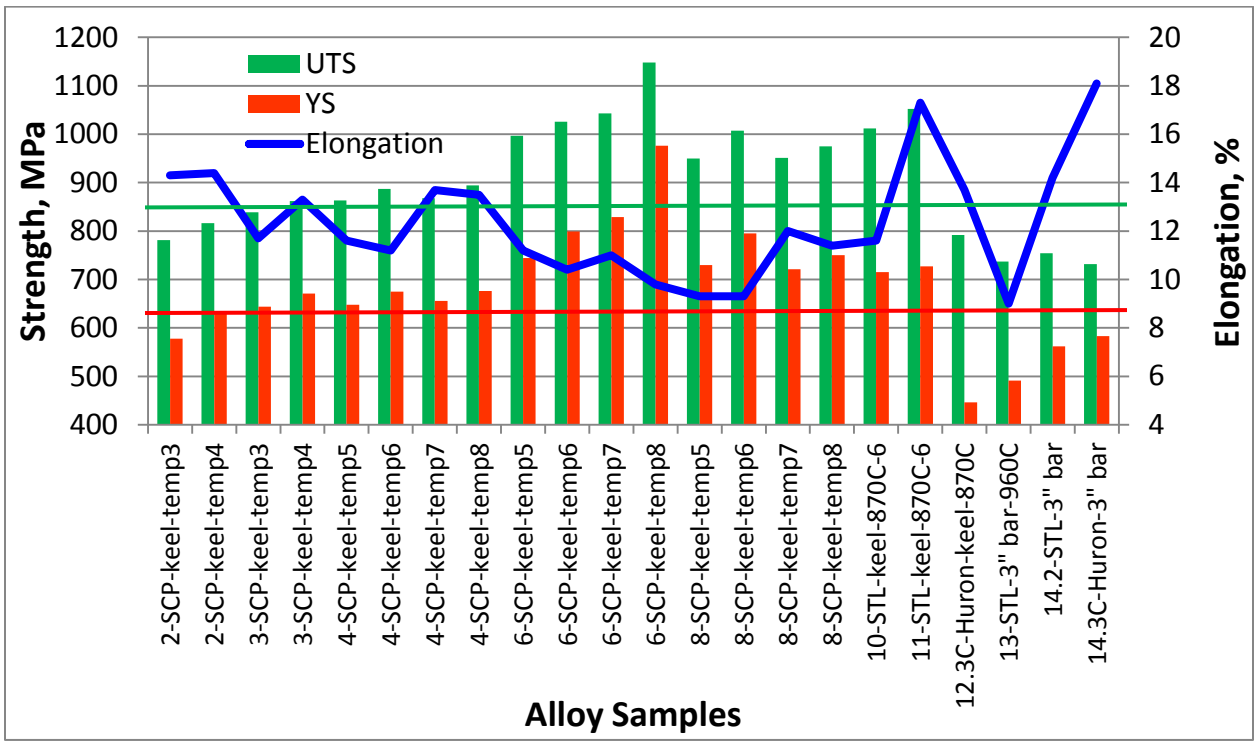

Figure 35. Most favorable tensile test results of samples from each alloy after different heat treatments

Process Design Concepts

The project team investigated the castability of multiple CAT and GM crankshaft designs. These crankshafts consisted of both current forged and cast ductile iron crankshafts. ICME process simulation tools were used to investigate a broad range of processing concepts. These concepts included casting orientation, various mold and core materials, and various filling and feeding strategies. Each crankshaft was first simulated without gating and risers, which is termed natural solidification. The natural solidification results were used as a baseline for strategy development of each concept. The goal was to identify the benefits and challenges of each concept and feed that information to designers to develop crankshaft designs more suitable for a given concept. The challenges identified also served as a basis for prioritizing focus areas for new process technology development specific to crankshafts.

The team investigated vertical orientation casting processes using a single riser on the end for several current crankshaft designs. For the vertical casting orientation, both gravity pouring and counter-gravity filling processes were examined. The counter-gravity process draws the liquid metal up into the mold cavity using a vacuum, which provides excellent flow control resulting in a low turbulence filling process. This is especially important for casting in the vertical orientation as the metal has to fall a long distance using gravity pouring techniques, leading to very high filling velocities and creating excessive turbulence and splashing.

A simulation was also run in which the crankshaft was rotated 180^{o} after counter-gravity filling was complete. The temperature contours in Figure 36 showed that when the casting was rotated after filling the riser had a higher temperature than the rest of the casting. The riser in the casting that was not rotated was at a lower temperature than the casting, which would lower its feeding efficiency.

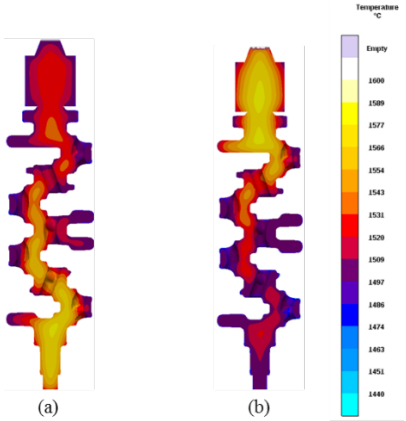

Figure 36: Temperature contour at the center of the vertically cast crankshaft. (a) No rotation after filling. (b) 180 degree rotation after bottom filling through the riser.

Figure 37 shows the porosity predictions for these two castings. There may have been less porosity in the top half of the casting for the rotated case; however, due to the complex geometry, the single top riser could not feed the entire casting and the total volume fraction of porosity was not significantly improved by rotation.

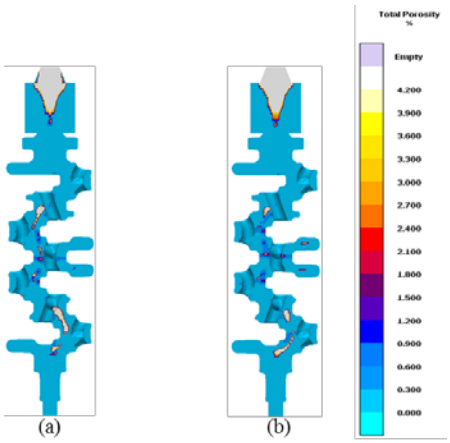

Figure 37: (a) Porosity contour of the vertically cast crankshaft that does not rotate after filling. Cut to show the center of the casting. (b) Porosity contour of the vertically cast crankshaft that rotates 180 degrees after filling. Cut to show the center of the casting.

In general, bottom filling the crankshaft in a vertical orientation showed the best filling; however, there were many challenges identified in feeding all the hot spots in a steel crankshaft casting in the vertical orientation. Casting the crankshaft in the horizontal orientation it was much easier to feed the numerous hot spots. The use of both highly conductive and insulating mold and core materials was also investigated, but a broad change of the mold or core material alone did not significantly improve the feeding challenges, and in some case a more conductive mold made the feeding conditions worse.

In order to validate the ICME process simulation tools, the team decided to prototype a crankshaft using a fully developed process that was predicted to be essentially free of macro-porosity defects and contain optimized amounts of micro-porosity. A General Motors small gas engine (SGE) crankshaft was selected for this case study. A mold design was developed using a simple end filling gravity casting approach with a horizontal crankshaft orientation. Several simulations were run to develop a feeding, riser, and chill strategy that predicted a crankshaft with minimal porosity.

Two sand molds were 3D printed at the University of Northern Iowa Additive Manufacturing Center, directly using the 3D model from the simulations. The sand molds consisted of four parts, a cope, a drag, the journal cores, and a filter access plug in the bottom of the drag. A chill was also utilized. The two prototype castings were poured at St. Louis Precision Casting Company using alloy 2. There were no visible surface defects and overall the castings looked very good. The castings were sent to Caterpillar where they were given a normalization heat treatment. After heat treatment, the castings were sent to Element Materials Technology for evaluation. X-ray radiography was conducted with the risers still attached. The riser piping (feeding) agreed very well with simulation predictions. Detailed correlation of the experimental and predicted results showed the simulations were very reasonable at predicting the location of porosity. See Figures 38 and 39 for examples of predicted versus actual macro-porosity and micro-porosity.

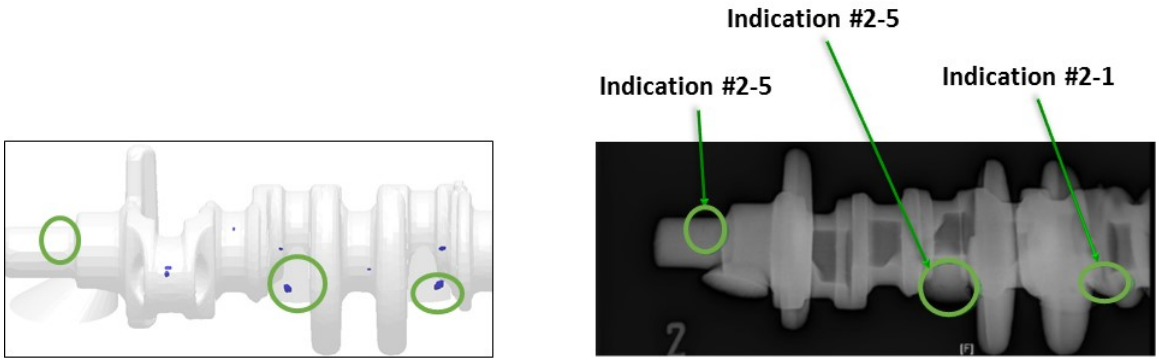

Figure 38: comparison of predicted macro-porosity and X-ray indications for GM crankshaft cast in alloy 2

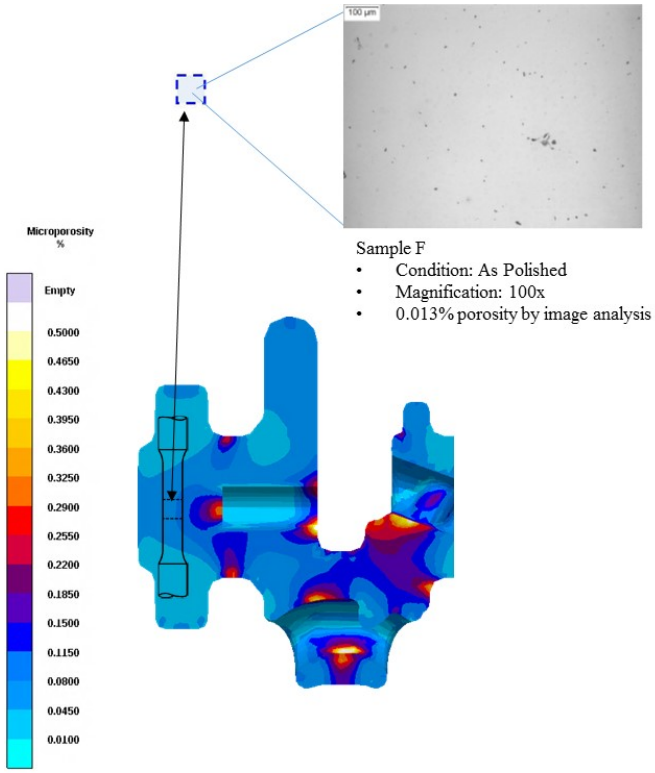

Figure 39: comparison of predicted and actual micro-porosity for GM crankshaft cast in alloy 2

Many inclusions and varying degrees of micro-porosity were observed in the test bar castings, so mold designs and filling methods were investigated that could produce cleaner steel castings.

The University of Iowa developed an experimental vacuum-assisted counter-gravity (VACG) system to further investigate the application of this process for cast crankshaft production. The VACG system, Figure 40, consisted of four major components, the vacuum pump, accumulator tank, pressure regulator, and vacuum chamber. The vacuum chamber, Figure 41, was a welded steel box with a lid,

which sealed to the chamber with a high temperature silicone rubber gasket.

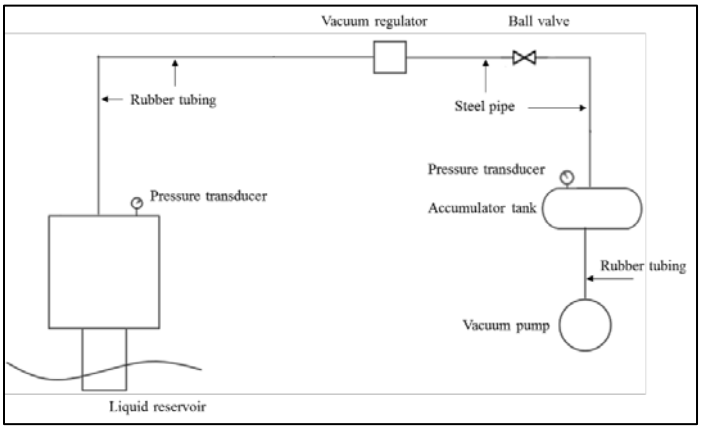

Figure 40. VACG system diagram.

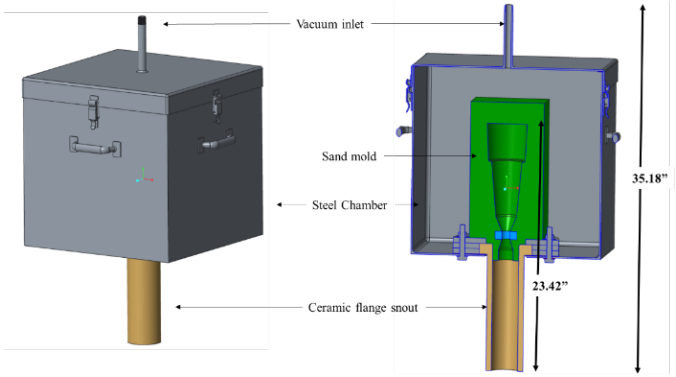

Figure 41. Vacuum chamber with internal components.

The VACG process operates as follows. With the ball valve in front of the accumulator tank closed, the vacuum pump draws air out of the accumulator, creating a lower vacuum than will be needed to draw liquid steel into the mold. When the pressure in the tank reaches a suitable range the ball valve is opened and the vacuum regulator controls the pressure inside the vacuum chamber. A sacrificial seal over the inlet to the ceramic snout allows a small vacuum to be drawn within the vacuum chamber. Next, the vacuum chamber's ceramic snout is lowered into the furnace melt, destroying the sacrificial seal, allowing liquid to rise into the sand mold within the vacuum chamber. The pressure in the chamber is regulated in a way that allows for the mold to fill completely and quiescently.

The geometry of the test casting that was to be used to validate the VACG system was developed by simulating filling and solidification with different inlet designs and time dependent pressure profiles. The top section of the part is based on the middle (2") test bar used for gravity casting alloy trials (see Figure 7). The effects of vacuum-assisted casting on metal quality were to be directly compared to gravity-pour castings that were discussed earlier in this report. The last week of September 2016, the University of Iowa successfully cast a steel bar using their VACG apparatus. That bar was X-rayed and die penetrant tested and found to appear clean regarding centerline shrink, while an identical bar cast in a traditional gravity poured sand mold showed some centerline shrink. The hope was that the VACG process would eliminate centerline shrink and the initial result validated the plan for further evaluation and experimentation with VACG casting.

Summary

In the project's first year (FY2014), encouraging material property results were achieved in a preliminary alloy casting trial, but the casting design used wasn't ideal for producing large numbers of samples to compare and characterize potential alloys. A vertically cast bar test casting design was completed for use in future alloy development experiments. Several virtual casting process studies were conducted and the team began to identify promising paths forward to successfully cast steel crankshafts. Design features were being identified that could improve the castability of steel alloys into complex shapes.

During the project's second year (FY2015), ICME based design of several alloy concepts was completed and a matrix of fourteen alloys for investigation was developed. A pattern and molding boxes for the vertically cast test bars was procured and casting trials were completed for 10 alloys. Preliminary structure-property characterization work was completed for 8 of the 10 alloys produced. A few of the concepts showed promise in meeting the property requirements for application as cast crankshafts. Keel block samples were cast and showed fewer casting related defects than the vertically cast test bars, which made it possible to compare the properties of various alloy chemistries and associated heat treatments. Several casting concepts were explored using ICME process simulations. A horizontal orientation sand casting process was fully developed for a GM small gas engine (SGE) crankshaft. Prototypes of the GM SGE crankshaft were made and reasonably validated the ICME predictions, from which the team gained confidence for designing and optimizing complex processes in the future.

In FY2016, remaining alloy concepts continued to be cast and characterized for structure-property relationships. Additional suppliers for alloy casting trials were identified that had better melting, treatment, handling, and pouring practices. The remaining alloy concepts required a ladle pouring process as special alloy and treatment additions were required to be done in the ladle rather than the furnace. The preference was for either a bottom or teapot style pouring ladle. After identifying a new supplier, alloy trials for the high-potential alloy candidates were repeated to evaluate the effects of various foundry practices on material quality, e.g. micro-porosity and inclusions.

In-depth microstructure characterization was carried out for each alloy at Element Materials Technology, Northwestern University, and Caterpillar. Correlation of the microstructures with ICME predictions were made and the models were updated to improve the predictive capabilities of the ICME tools. Dilatometry experiments were conducted on a few of the high-potential alloy candidates to develop TTT and CCT diagrams to improve the ICME models and facilitate a better understanding of the phase evolutions. Additionally, "in-situ" X-ray diffraction experimental methods were explored at Argonne National Lab to further develop CCT and kinetic models for the phase evolutions. Updated ICME models were used by Northwestern and Caterpillar to further optimize the high-potential alloy concepts, including compositions and heat treatments.

Micro-porosity has been shown to significantly affect critical properties of the cast material. Characterization work was done to further quantify the micro-porosity in the samples cast to date. Micro-porosity predictions were made using ICME simulations for the test bars, keel blocks, and crankshaft castings. Those predictions were compared with the actual castings to determine if the micro-porosity levels could be accurately predicted and work began to see if the micro-porosity predictions could be correlated to material performance. A criteria for the allowable level of predicted micro-porosity should be developed for use in cast steel crankshaft process development. It was

planned that Caterpillar would update the micro-porosity model in its internal solidification software, SolCAT3D, in order to evaluate the effects of nitrogen levels in the liquid steel on micro-porosity formation during solidification.

Casting process concepts were explored through both simulation and experiments. A detailed inspection plan for the two prototype crankshafts produced was developed and the results were used to correlate with the simulation models. The vacuum-assisted counter-gravity (VACG) system developed was tested using water as the fluid by replacing the ceramic flange snout with PVC piping. The water experiment was used to check for issues ahead of developing a plan for the first liquid steel experiments with the apparatus. Work began to compare the metal quality from the VACG experiments to traditional gravity cast samples to quantify the benefits of the clean steel casting process.

Detailed data analysis took place in FY2016 and the following observations were made:

- Of the specimens produced, cast keel blocks have the best properties, especially elongation.
- Tensile bars excised from the mid-radius section of 3" bars had the best properties of the test bars samples, and those properties were comparable to corresponding keel block samples, while samples from the centers of 1" and 3" bars exhibited low elongation, most likely due to higher levels of micro-porosity.
- Post-normalization temper treatments indicated a weak effect at 225^{o}C, but a strong effect at 500^{o}C, which led to a slight variation of UTS, certain increase of YS, and significant increase of elongation.
- Alloys 3, 4, 6, and 8 could meet material property goals (UTS>850 MPa, YS>615 MPa, elongation>10%) after appropriate normalization and temper treatments.
- Alloys 10 and 11 could also meet the goals, but they may not have sufficient hardenability for bearing journal induction hardening due to low carbon concentrations.
- Alloys 12, 13, and 14 have low yield strengths for the heat treatments considered and could not meet the goals.
- The GM crankshafts cast in alloy 2 at St. Louis Precision Casting on 6 August 2015 were normalized at 900^{o}C for 3 hours and cooled in still air. Three tensile bars were excised from one of the crankshafts and had the very promising properties shown in Table 4 (reference Figure 9). Note that keel block legs cast in alloy 2 in early and later stages of the project showed some promise, but generally the results from keel blocks didn't come close to the combination of UTS and elongation properties measured in the bars excised from the crankshaft casting.

Based on high-potential alloy and process concepts identified, work was planned to develop new crankshaft design concepts that take advantage of the casting process and material properties to minimize the component weight while optimizing the castability. A scaled model (single-throw) version of the GM SGE crankshaft was designed to be used in casting process and component design development work. It was planned to work with this single-throw crankshaft design in casting process simulations to optimize the gating and risering design and incorporate design features to optimize structural performance and castability in an iterative development process. The University of Iowa was provided GM's final single-throw crankshaft design on 4 October 2016 so they could begin development of a sprue, runner, gate, and riser design for both traditional sand casting and for casting in their VACG apparatus. The intention was to compare castings from the two processes to determine if the VACG process offered any benefits, but the project was terminated before that could happen.

During October 2016, GM developed a very detailed budget and time line planning document to help ensure that planned casting pouring, machining, processing, tuning fork fatigue testing (bench testing), heat treatment development work, and ultimately engine durability testing of crankshafts would happen within the time remaining for the project.

In a process that started mid-August 2016, there were several revisions of the statement of requirements for producing the GM SGE crankshaft molds, keel blocks, and nominal 2 inch diameter bars to be used for evaluating five alloys proposed as a result of earlier alloy development research. The requirements continued to evolve as project work continued to generate new knowledge and through discussions with suppliers that resulted in improvements to planned work and data generation. The University of Northern Iowa Additive Manufacturing Center was selected and contracted to provide 3D printed molds for additional prototype GM SGE crankshaft castings to be made from one of the five high-potential alloys. Southern Cast Products was contracted to pour the castings from the five most recent high-potential alloys.

1 November 2016 Element Material Technology results became available from 32 tensile bars representing various combinations of alloy chemistry and heat treatment that were prepared by Caterpillar to help narrow the field in the alloy development portion of this project. These 32 specimens represented alloy development chemistries 2, 3, 4, 6, 8, 10, and 11. Generally, it was found that a post-normalization temper at about 500°C greatly increased the material yield strength and elongation. These results were used by Caterpillar and Northwestern University to develop the most recent five high-potential alloy chemistries that were poured during November 2016 at Southern Cast Products, namely alloys 4A, 4B, 6A, 10A, and 11A.

The heats at Southern Cast Products were designed to produce specimens to evaluate alloys 4A, 4B, 6A, 10A, and 11A and ultimately to cast, machine, and process about 40 SGE crankshafts to be used for tuning fork fatigue studies, induction hardening studies, and material property studies. The intent of the planned tuning fork fatigue studies was to assess the effects of micro-porosity on fatigue life. Prior to casting all 40 GM crankshafts, initially only 4 crankshafts (2 molds) were poured to make sure there were no process, mold, or other unforeseen problems. Those crankshafts were laser scanned for dimensional checks before and after heat treatment and then sent to Element Materials Technology for quality and metallurgical characterization. The dimensional scan results indicated that not enough shrink allowance was used and the castings wouldn't clean up during machining. This dimensional problem will need to be corrected by adding more shrink allowance.

14-15 November 2016 Southern Cast Products poured keel blocks, in addition to the 4 GM crankshafts, to be used for optimizing base material properties through various normalization and temper heat treatments of the five high-potential near final alloy chemistries, alloys 4A, 4B, 6A, 10A, and 11A. Southern Cast Products also poured nominal 2 inch round bars in the five high-potential alloys to be used in studies planned to optimize surface material properties through various induction hardening set ups. The GM SGE crankshafts were poured in alloy 4A. The intention was to pour 12 keel blocks and 6 round bars with each chemistry heat. Here is a list of the castings that were successfully poured: Alloy 4A - 12 keel blocks, 6 round bars, 4 crankshafts; Alloy 6A - 12 keel blocks, 6 round bars; Alloy 10A - 12 keel blocks, 3 round bars; Alloy11A - 4 keel blocks, 3 round bars; Alloy 4B - 8 keel blocks, 3 round bars. The higher vanadium content of heats for alloys 10A and 11A proved to be problematic and residual effects in the pouring ladle may have been problematic for the alloy 4B heat poured after them. The pouring temperature for the heat of alloy 10A was too low, but it is not fully understood why all of the last three heats (10A, 11A, and 4B) experienced molten metal fluidity and mold filling problems.

Recommended heat treatments were developed by Caterpillar and Northwestern University for alloys 4A, 4B, 6A, 10A, and 11A poured into keel blocks at Southern Cast Products during November 2016 and those heat treatments were performed by Caterpillar during December 2016.

2 December 2016 detailed instructions were sent to Element Materials Technology to X-ray the 4 crankshafts cast at Southern Cast Products and run complete chemistries on the final heat chemistry samples. There were a few minor porosity indications on the crankshaft X-rays, but nothing significantly different than expected from the casting simulation work. 15 December 2016 additional instructions were sent to Element to obtain surface hardnesses and then section two of the crankshafts and perform die penetrant tests. It was also requested that three tensile bars be excised from one of the crankshafts for metallurgical characterization and material property determination. As of the date of the contract termination notice those test results were not available.

The last week of September 2016, the University of Iowa successfully cast a steel bar using their VACG apparatus. That bar was X-rayed and found to appear clean regarding centerline shrink. On 3 November 2016 Element was asked to section and perform die penetrant testing to compare a bar cast in a traditional gravity poured sand mold and the VACG cast bar. The VACG cast bar was clean while the traditionally cast bars showed some centerline shrink, which was the hope and validated the plan for further experimentation with VACG casting. 2 December 2016 instructions were sent to Element for further sectioning these two castings for a detailed evaluation of micro-porosity in various bar cross sections. As of the date of the contract termination notice those test results were not available.

Project Successes

- Potential alloys were developed that can meet the project material property goals (UTS>850 MPa, YS>615 MPa, and elongation>10%) with appropriate normalization and temper treatments. For the alloys considered, post-normalization temper treatments proved to be necessary to achieve the desired yield strengths and elongations and appropriate heat treatments were designed using ICME tools.
- The experimental data of all the alloys were analyzed in combination with ICME tools to establish chemistry-process-structure relations.
- GM small gas engine (SGE) crankshafts were successfully cast using two different sprue, runner, gate, riser, chill designs. Both mold designs cast the crankshaft horizontally and one fed the casting through a riser on the flange end and the other fed the casting from the bottom (lowest points) at multiple locations. The mold yields were on the order of 33%. The casting simulations reasonably predicted the macro-porosity and micro-porosity in the casting. Casting finishing (e.g. riser removal) remains a cost challenge.
- Casting process simulations and ICME tools were proven to be reasonable predictors of real world results.

Future work

There were many milestones in this project that were left incomplete and that warrant further investigation and development, including:

- As-cast and heat treated test specimens for high-potential alloys 4A, 4B, 6A, 10A, and 11A should be metallurgically characterized and compared to ICME predictions to see if they satisfy

the project's material property goals of UTS > 850 MPa, YS > 615 MPa, and elongation > 10% and for use in further revising ICME tools.

- Many of the microstructures produced by these alloys proved very difficult to characterize and more detailed metallography characterization would be in order.
- Since heat treatments were able to significantly increase the yield strength and elongation properties of the alloys considered even though those alloys contained micro-porosity of varying levels, the relationship between micro-porosity and those properties needs further examination.
- Further iterative development work should be done to optimize the alloy chemistry and heat treatment and update ICME tools, particularly in regard to producing a machining friendly structure and one that has sufficient surface hardness or is surface hardenable. The remaining alloy concepts should be cast and structure-property characterization completed. CCT and TTT curves for high-potential alloy concepts should be developed.
- Enough test specimens should be produced to generate statistically valid material property / characterization data for the final alloy choices.
- The effects of vanadium additions on the melting temperature and castability of similar alloys should be fully investigated.
- An accurate pattern making shrink rule needs to be developed for the developed alloy.
- The effects of residual micro-porosity on fatigue life need to be understood through component bench testing and limits for allowable micro-porosity in cast steel crankshafts need to be developed.
- The response of cast steel crankshafts to induction hardening and fillet rolling need to be understood as a function of alloy composition, especially carbon. Can an alloy be developed that does not require surface hardening of the bearing journals, but that is still economical to machine?
- The process and cost impacts of machining cast steel alloys likely to contain bainite throughout the component need to be understood.
- Further work is necessary to develop a crankshaft design and associated material, casting process, and mold design that satisfies the product performance criteria while improving the component mass, mold yield, and casting finishing cost, including: degating and riser removal, machining, fillet rolling, post-casting heat treatment complexity, etc. How far could the University of Iowa vacuum-assisted counter-gravity (VACG) process go toward achieving such improvements over more traditional sand casting? Caterpillar had started some work to take advantage of the material properties of high-potential alloys to optimize mass and castability of one of their crankshafts, but GM had only worked with existing product geometries at the point of project termination.
- Once a final optimized product is developed, component testing needs to occur through engine durability testing.

References

None

Publications and Presentations

None

Acknowledgement

This material is based upon work supported by the Department of Energy under Award Number(s) DE-EE006428.

Disclaimer

This report was prepared as an account of work sponsored by an agency of the United States Government. Neither the United States Government nor any agency thereof, nor any of their employees, makes any warranty, express or implied, or assumes any legal liability or responsibility for the accuracy, completeness, or usefulness of any information, apparatus, product, or process disclosed, or represents that its use would not infringe privately owned rights.

Reference herein to any specific commercial product, process, or service by trade name, trademark, manufacturer, or otherwise does not necessarily constitute or imply its endorsement, recommendation, or favoring by the United States Government or any agency thereof.

The views and opinions of authors expressed herein do not necessarily state or reflect those of the United States Government or any agency thereof.